



Low Temperature Electrocatalysts for Green Hydrogen and Ammonia

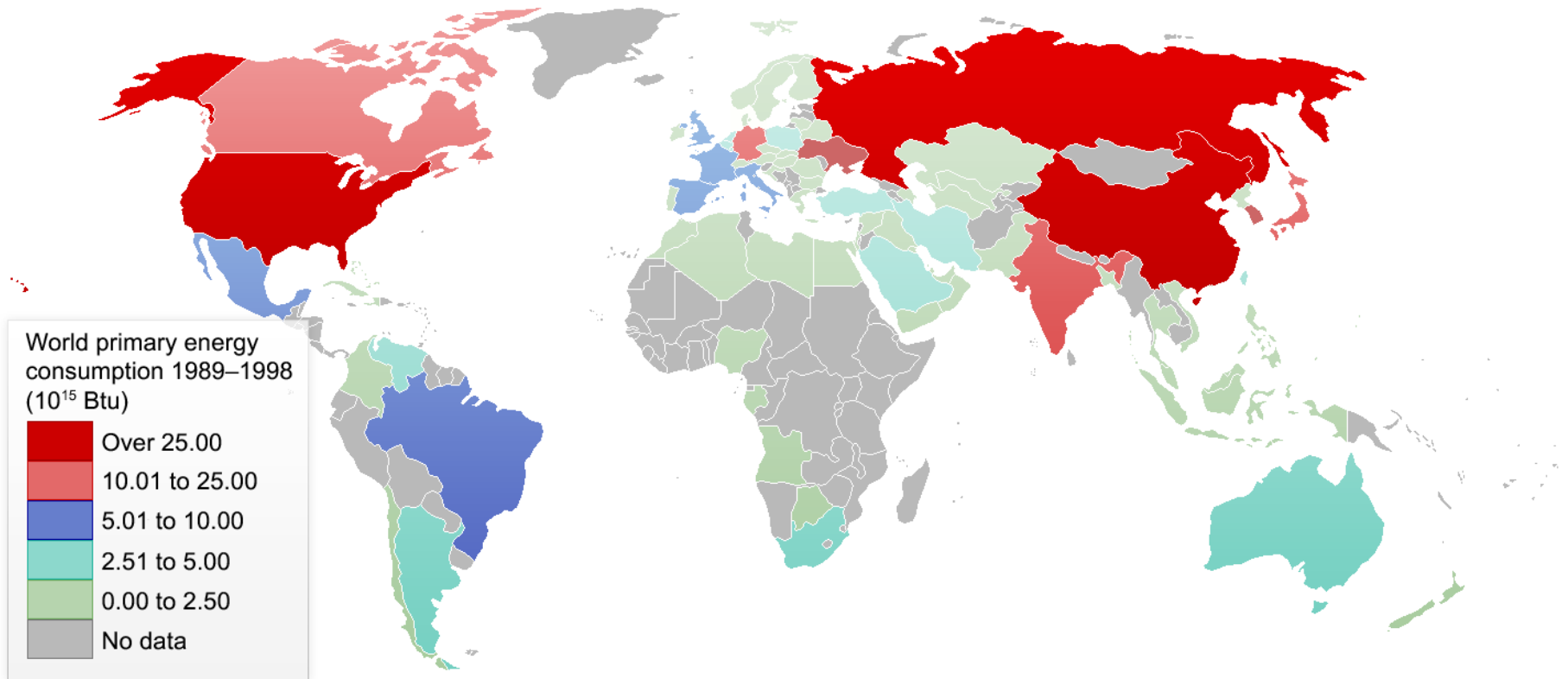
Keith J. Stevenson

Skoltech

November 15, 2021

World Energy Demand

Energy consumption predicted to increase 56% from 2010-2040



Require 30-40 TW to support >10 billion by 2050

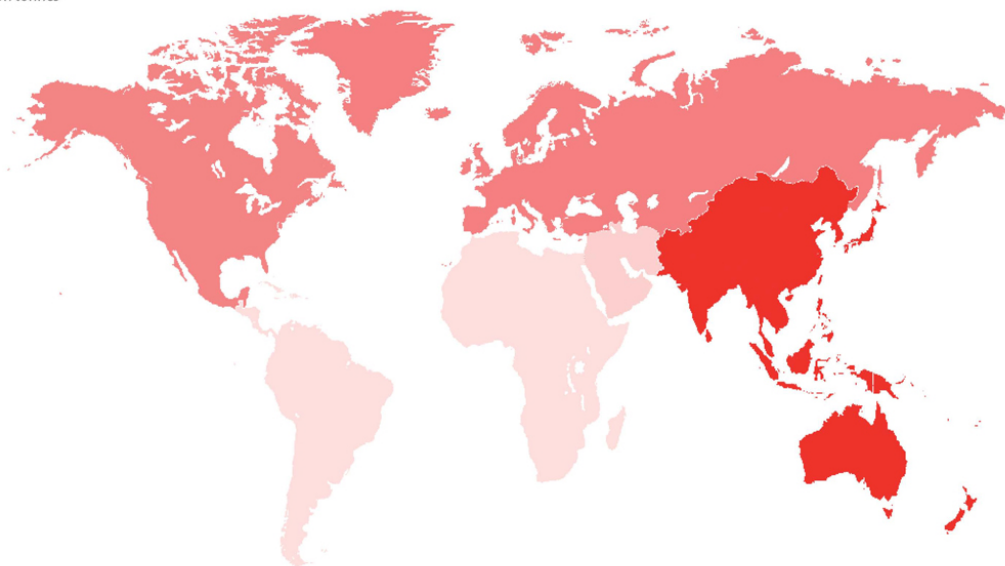
Global Greenhouse Gas Emissions

Emissions predicted to rise considerably

By Consumption

World CO2 emissions from consumption of energy

Million tonnes



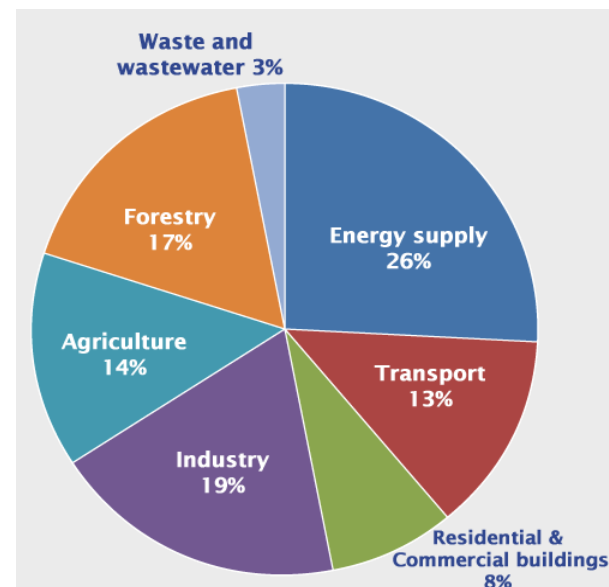
CO2 emissions from consumption of energy
by region

Million tonnes oil equivalent

Share of total, %

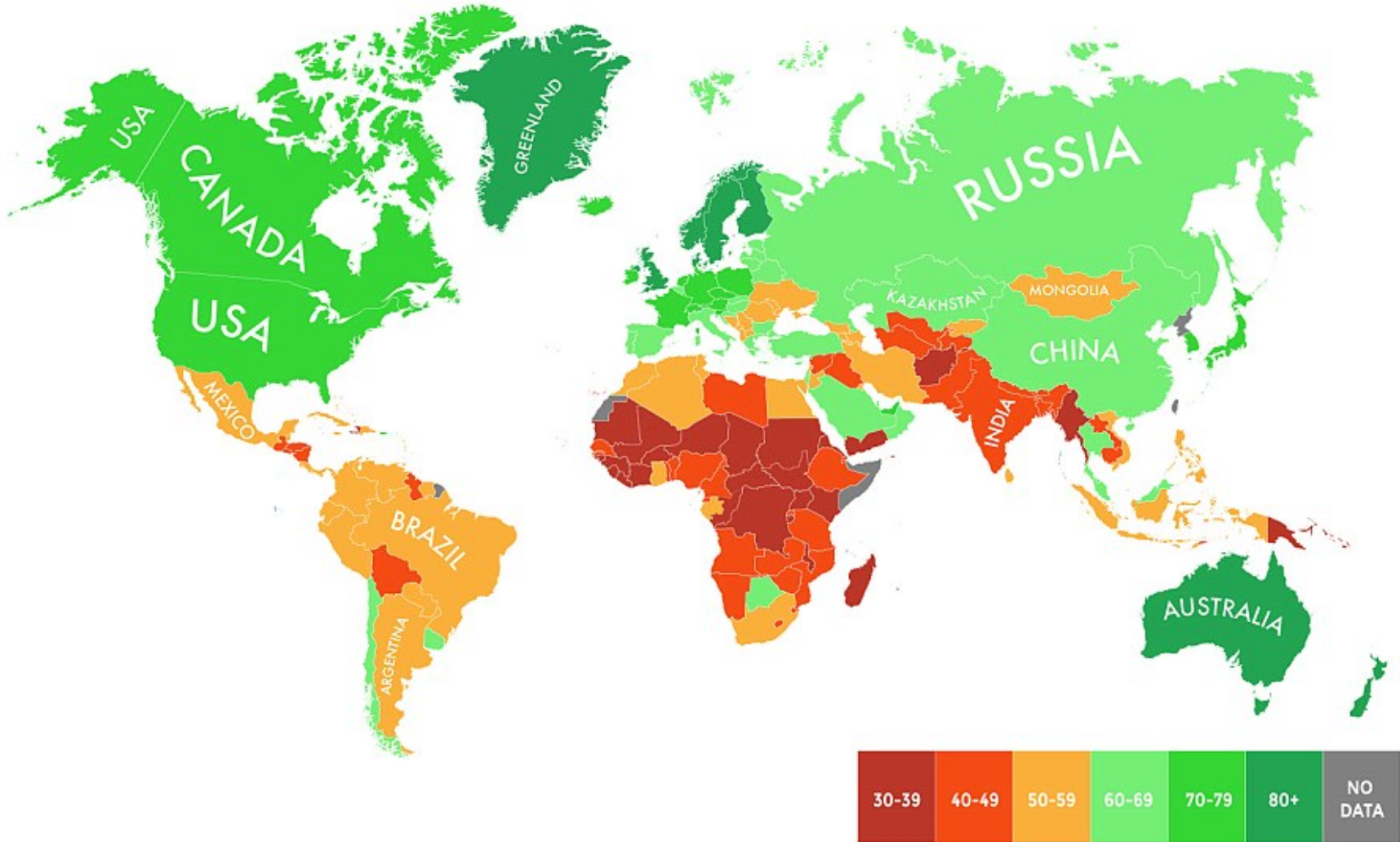
North America	6 410.54	21.1%	Total World	30 398.42
S. & Cent. America	1 219.78	4.1%		
Europe & Eurasia	6 668.33	21.9%		
Middle East	1 714.03	5.6%		
Africa	1 121.59	3.7%		
Asia Pacific	13 264.09	43.6%		

By Source



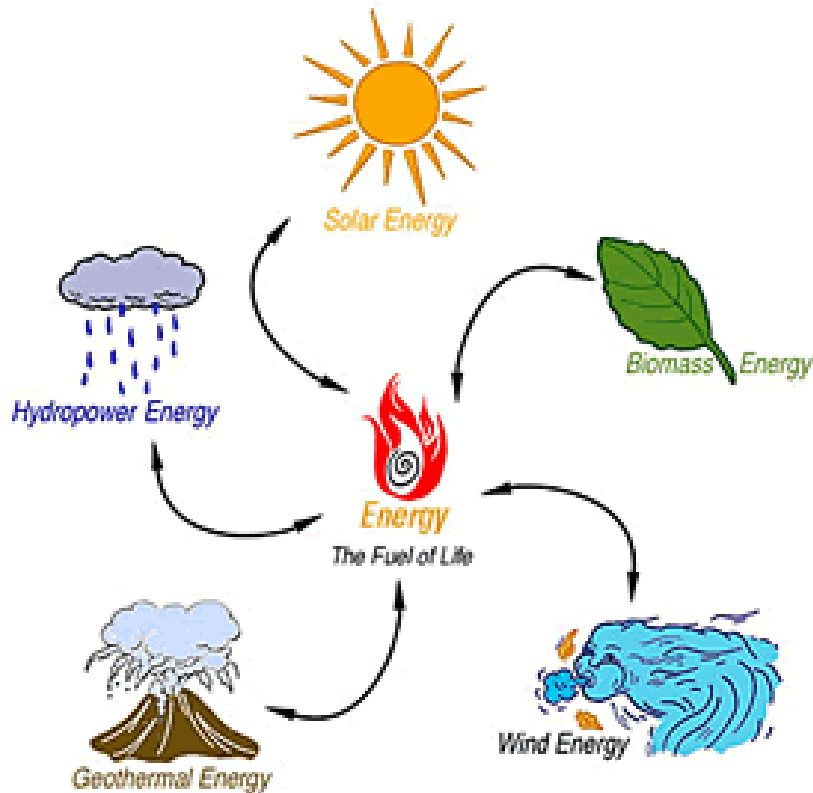
Countries Best to Cope With Climate Change

Ranked by “Vulnerability” and “Readiness”

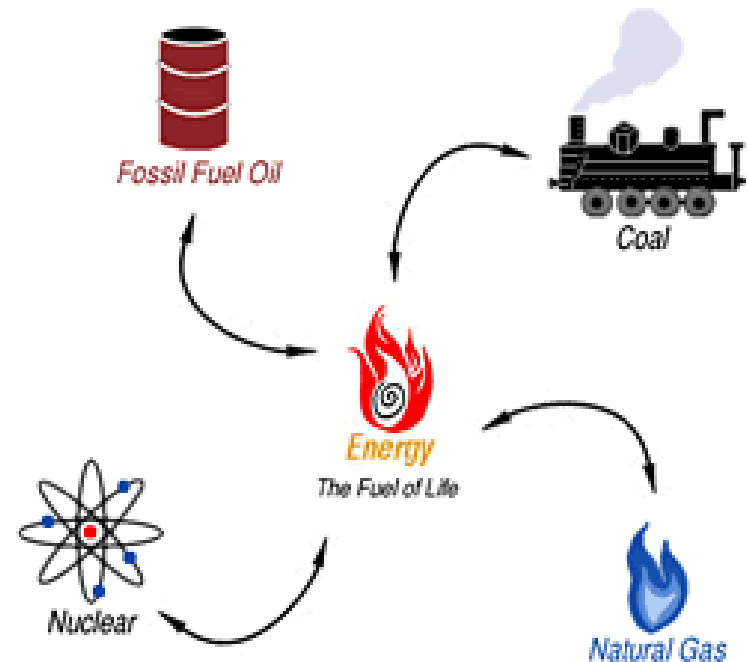


Alternative Energy Versus Conventional Energy

Renewable Energy



Non-Renewable Energy



Closed Loop, Carbon Neutral Versus Open Loop, Carbon Emission

Grand Challenges for Energy Sustainability

Carbon Free Energy

- Require 30-40 TW to support >10 billion by 2050.
- **Need new catalysts to support a mix of alternative energy sources.**

Main chemical transformations:

Methane Activation to Methanol: $\text{CH}_4 + \frac{1}{2}\text{O}_2 \rightarrow \text{CH}_3\text{OH}$

Direct Methanol Fuel Cell: $\text{CH}_3\text{OH} + \text{H}_2\text{O} \rightarrow \text{CO}_2 + 6\text{H}^+ + 6\text{e}^-$

CO_2 (Photo)reduction to Methanol: $\text{CO}_2 + 6\text{H}^+ + 6\text{e}^- \rightarrow \text{CH}_3\text{OH}$

H_2/O_2 Fuel Cell: $\text{H}_2 \rightarrow 2\text{H}^+ + 2\text{e}^-$; $\text{O}_2 + 4\text{H}^+ + 4\text{e}^- \rightarrow 2\text{H}_2\text{O}$

(Photo)chemical Water Splitting: $2\text{H}^+ + 2\text{e}^- \rightarrow \text{H}_2$; $2\text{H}_2\text{O} \rightarrow \text{O}_2 + 4\text{H}^+ + 4\text{e}^-$

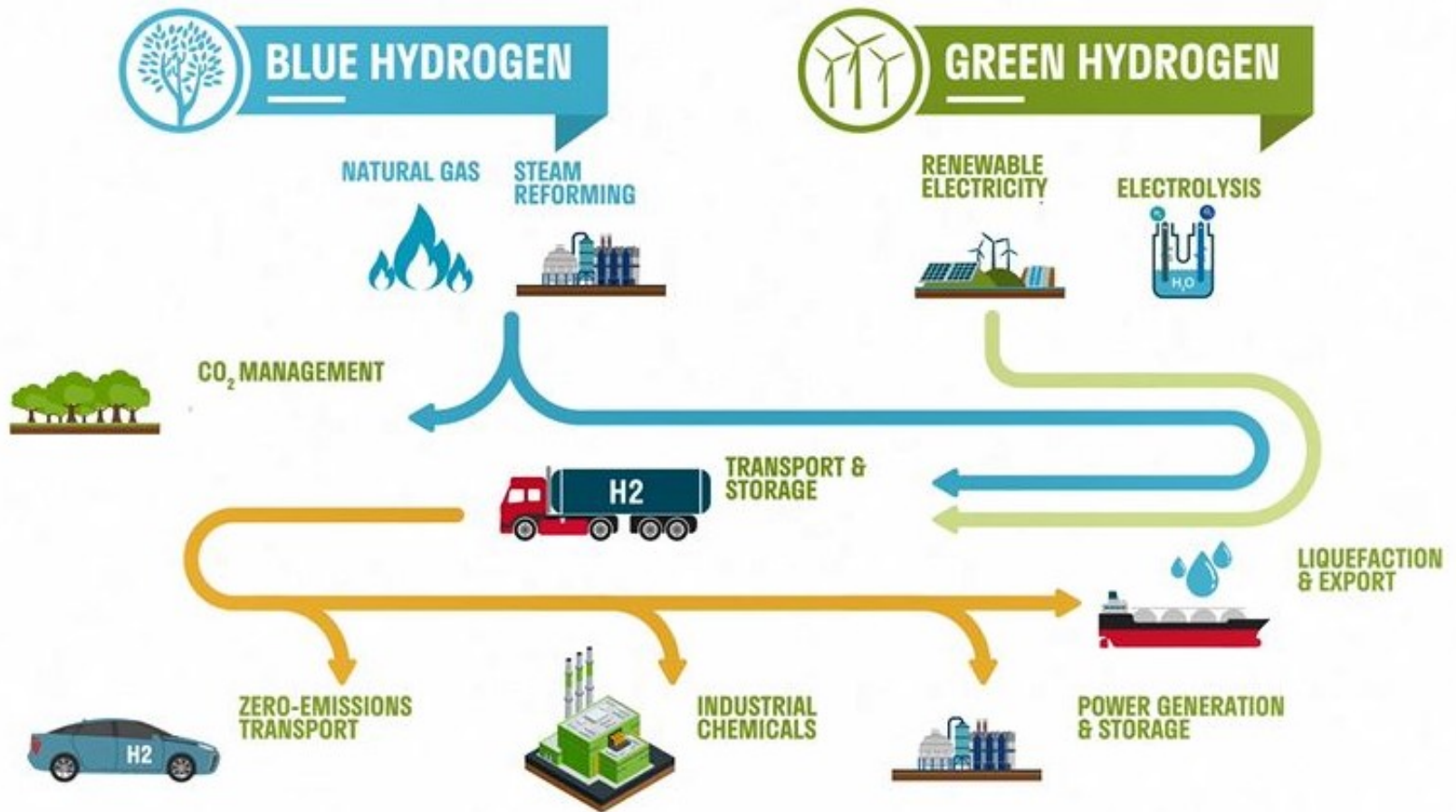
Dinitrogen to Ammonia: $\text{N}_2 + 6\text{H}^+ + 6\text{e}^- \rightarrow 2\text{NH}_3$; $\text{N}_2 + 6\text{H}_2\text{O} + 6\text{e}^- \rightarrow 2\text{NH}_3 + 6\text{OH}^-$

Strategy for Russia: Key Points from President Putin's Speeches 2021

- Reduce methane emission, eliminate gas flaring
- Energy efficiency across sectors
- CCUS from all sources
- Hydrogen as energy storage and source
- Establish carbon credits market
- Develop international monitoring system on GHG emissions using AI on data from satellites and ground measurements of CS
- Carbon sequestration in forests, capacity 2.5Bt CO₂
- Russia is closer to 1990 baseline than others
- Nuclear power is green energy
- Green investments welcome in Russia



Sustainable Hydrogen



Holy Grail: Sustainable Hydrogen and Ammonia

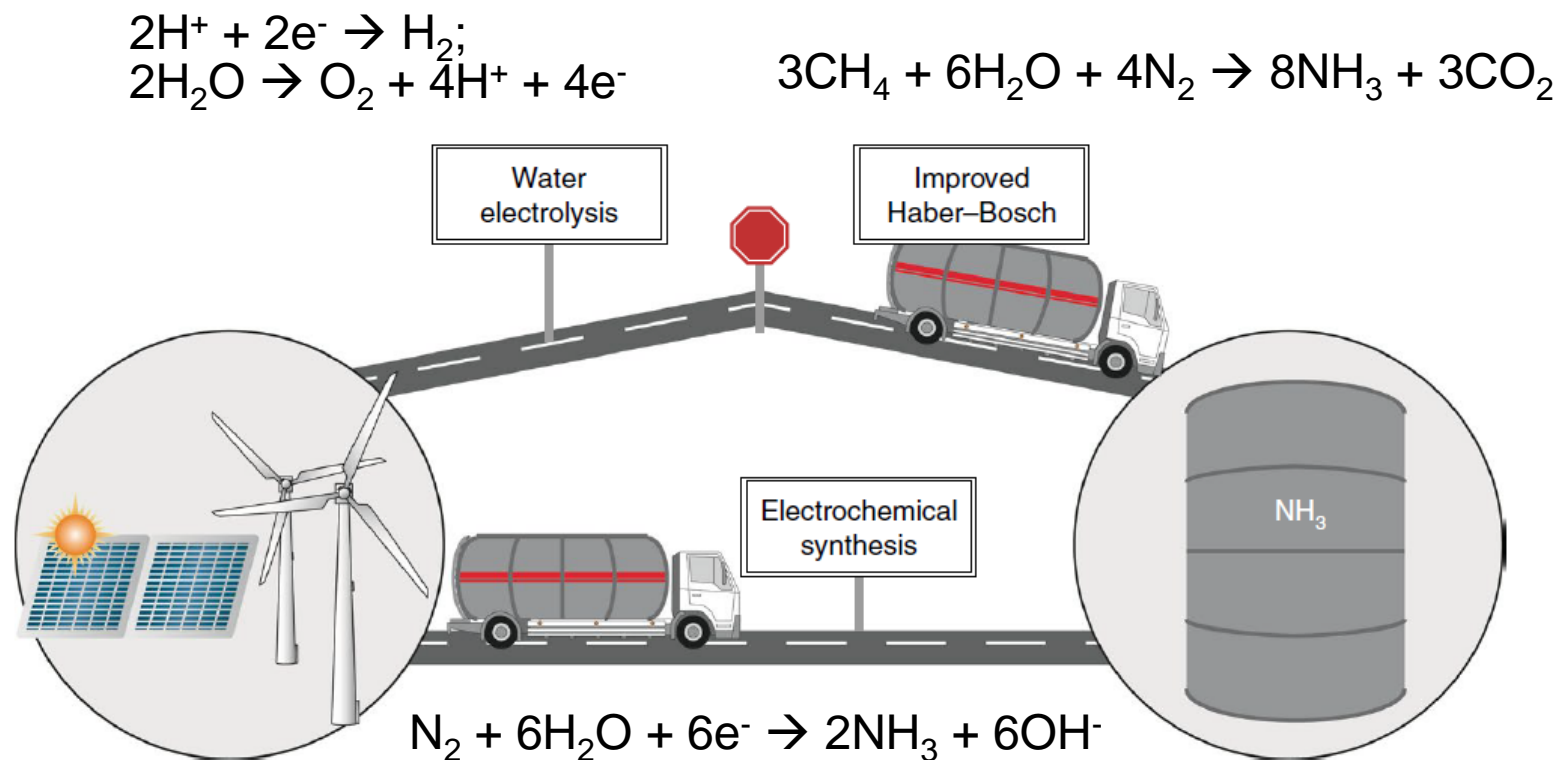
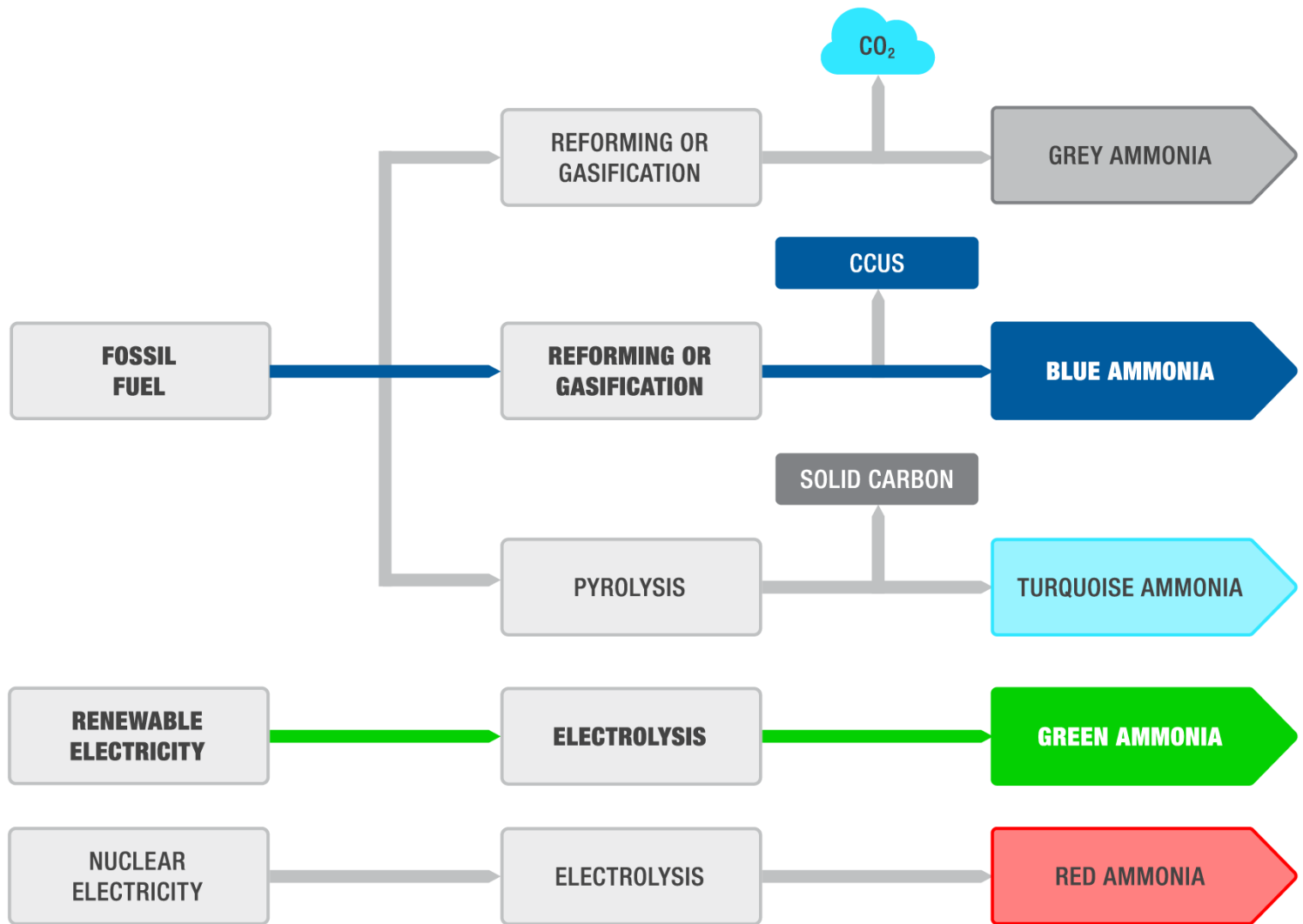


Fig. 1 | Pathways to renewable ammonia. Water electrolysis combined with the improved Haber-Bosch process (scenario A) and direct electrochemical synthesis (scenario B).

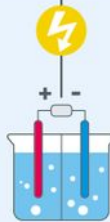
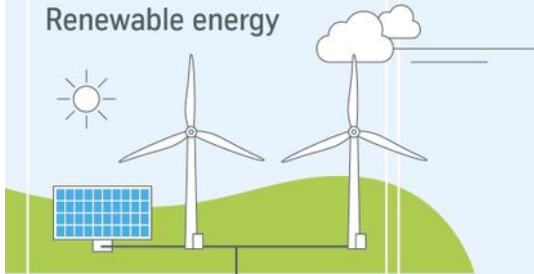
170 Million tons of NH₃ produced per year

1.5% of global total CO₂ emissions (2.9 ton CO₂ per NH₃)



Production

Renewable energy



Electrolysis

Transformation

1st stage transformation

2nd stage transformation

Green ammonia

Methanol

Further transformation

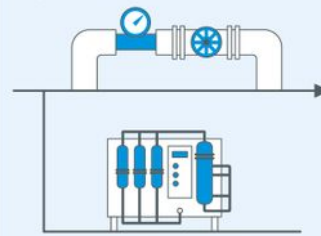
Synthetic fuels

Sustainable CO₂ capture

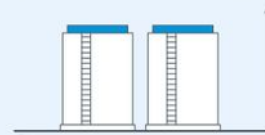


Transport

Pipeline



Ammonia cracking



Storage

Shipping



Trucks



End use

H₂ Heating



H₂ Industry

Steel industry



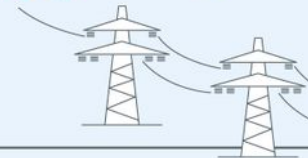
Chemical industry



Refineries



H₂ **NH₃** **MH** Power generation

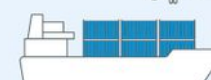


H₂ **NH₃** **MH** Transport

Aviation



Shipping



Rail



Cars



Trucks



Buses



Russia Focused On Export of Hydrogen and Ammonia

Future export oriented hydrogen & ammonia production sites in Russia: past & ongoing studies



Low Temperature Electrocatalysis for Green Generation of Hydrogen and Ammonia

Areas of focus:

Room Temperature Electrocatalysis for (OER, HER)

Electrochemical Oxidation of Hydrogen carriers, (Urea, MeOH)

Electrochemical Reduction of Nitrogen to Ammonia

Electrochemical Valorization of Waste (HMF, Furfural, Glycerol, Ligin)

Electrochemical CO₂ Reduction to Ethylene?

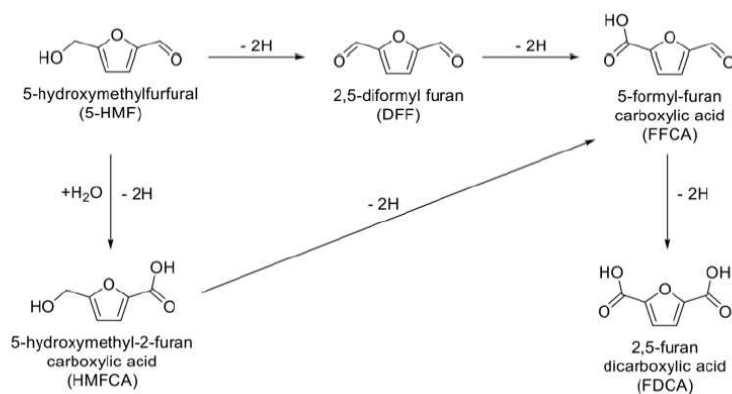
Alkaline Fuel Cells

Alkaline Electrolyzers

Skoltech CEST Faculty and Researchers

Stevenson, Abakumov, Nikitina, Levchenko, Akseyov,

Artemov, etc



Scheme 1. Value-added products derived from the oxidative upgrading of HMF.

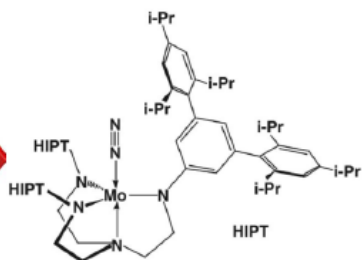
Five Broad Classes of Catalysts



Biocatalysts
e.g. enzymes

H₂O oxidation in photosynthesis

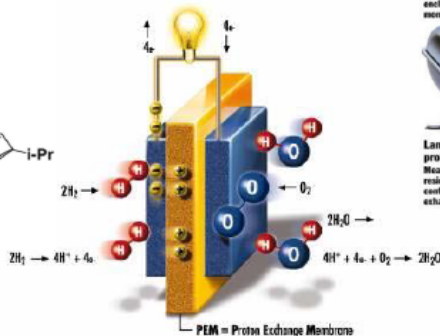
H⁺ and e⁻ transfers
Ambient Temp
Ambient Pressure
Liquid (aqueous)



Homogeneous Catalysts
e.g. transition metal complexes

Fine chemicals
Olefin metathesis

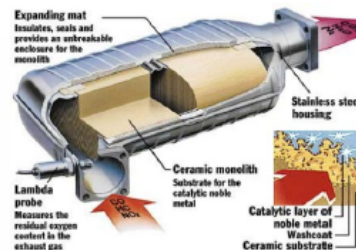
H⁺/e⁻, thermochemical
Low-Intermediate T's
Wide range P's
Liquid (aq. or non-aq.)



Electrocatalysts
e.g. Pt nanoparticles

Fuel Cells
Water electrolysis

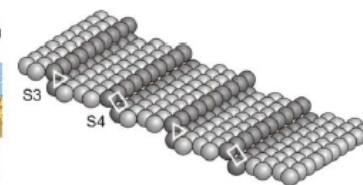
H⁺/e⁻, thermochemical
Wide range of Temps
Wide range P's
Liquid (aq. or non-aq.)



Conventional Heterogeneous Catalysts
e.g. Rh nanoparticles

Catalytic converters
NH₃ synthesis

Thermochemical
Wide range of Temps
Wide range of P's
Gas or liquid-phase

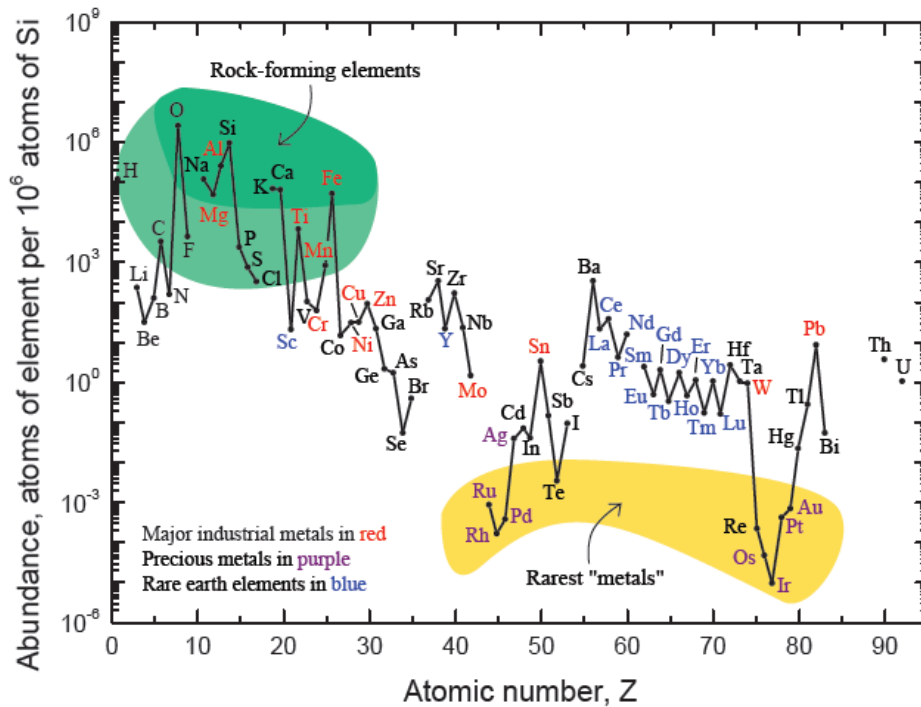


Ultra-high Vacuum (UHV) Surface Science
e.g. Ru(109)

Fundamental studies
Adsorption, desorption, reaction

Thermochemical
Wide range of Temps
Very low P (vacuum)
Gas-on-surface

Use of Rare Elements in Modern Technologies



- Chemical catalysis
- Electronics
- Batteries, Fuel & Solar Cells
- Petroleum refining
- Catalytic convertors
- Metal refining
- Glass polishing



Anode for NMH batteries;
about 10 —15 kg La per vehicle



Permanent Nd magnets

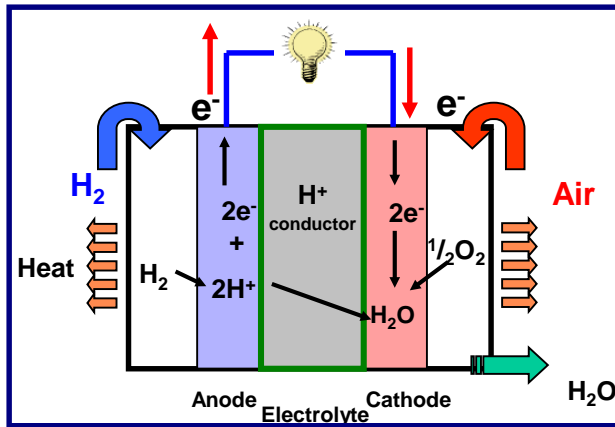


Tr, Eu, and Yt are the
blue, green, and red
phosphors used in
many light bulbs,
television, etc...

Electrochemical Energy Technologies

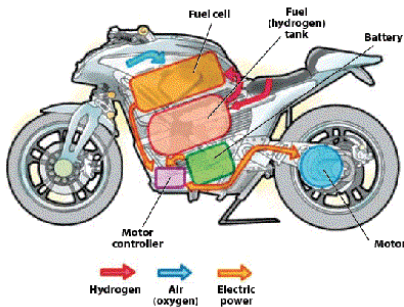
Fuel cells, batteries, supercapacitors (electrochemical)

Fuel Cell

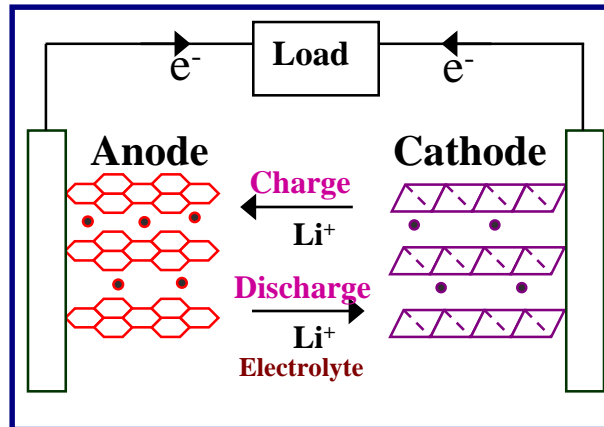


Conversion Device

Portable, transportation, & stationary



Battery

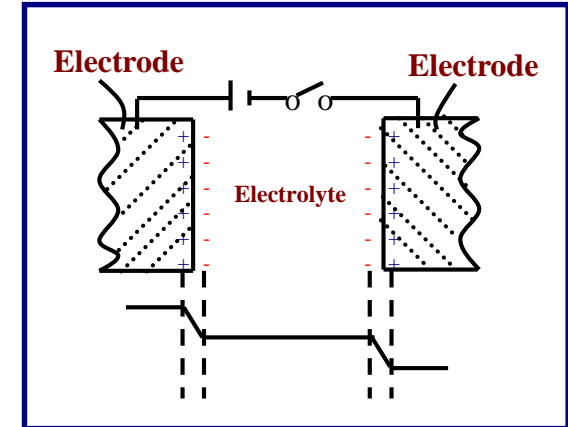


Storage Device

Portable & transportation

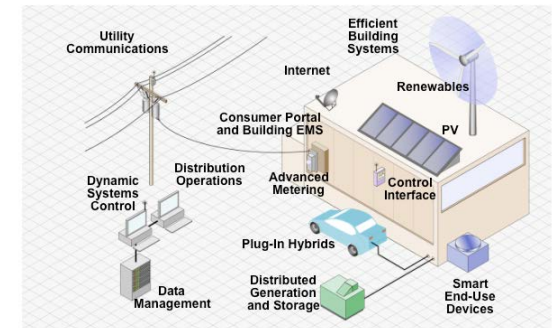


Supercapacitor



Storage Device

Portable & transportation



• Chemical energy directly into electrical energy – clean energy technologies

Electrochemical Power Sources Versus Combustion Engines

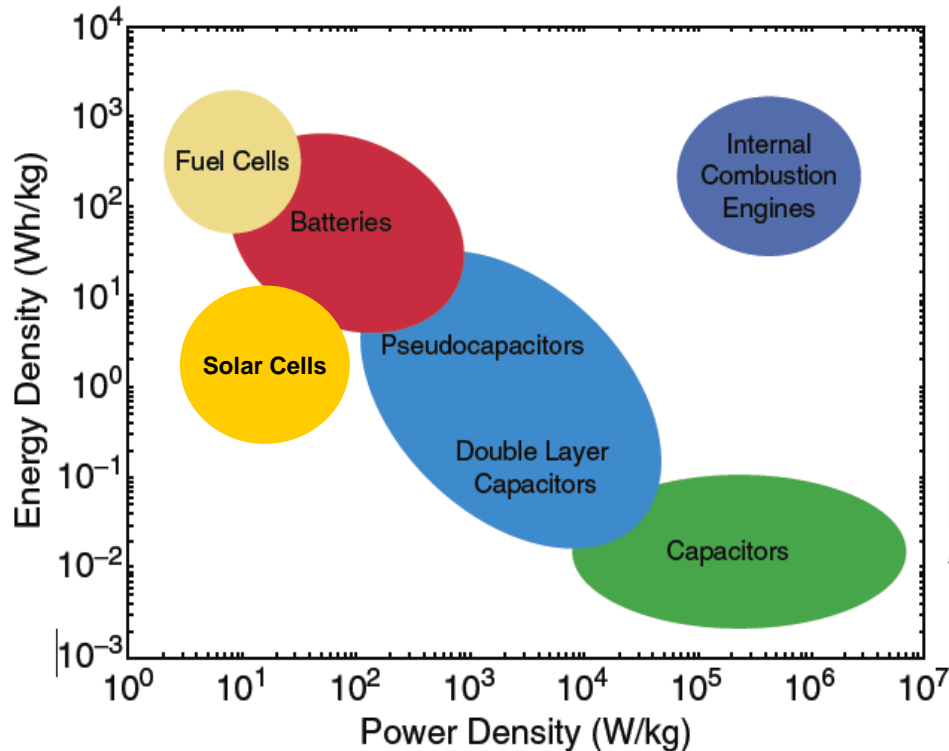


Table I: Energy Output of Electrochemical Devices and Petroleum.

Energy Source	Energy Output (kWh/kg)
Supercapacitors	0.01
Lithium battery	0.8
Hydrogen fuel cell	1.1
Gasoline	6.0 ^a

^aAssuming 30% combustion efficiency.

Electrochemical Energy Storage Options

Secondary batteries

- Stationary electrode materials
- Mature technology (lead acid, NiCd, NiMH, NaS)
- Emerging technologies (NaMCl₂, Li-ion)
- New chemistries (Li-air, Li-S, Zn-air)



NGK 34 MW NAS alongside 51 MW Wind Farm

Source: <http://www.ngk.co.jp/english/products/power/nas/>

Redox flow batteries

- Flowing electrode materials
- Mature technology (zinc-bromine, all-vanadium)
- Emerging technologies (cerium-zinc, iron-chromium)
- New chemistries (vanadium-bromine, soluble lead)

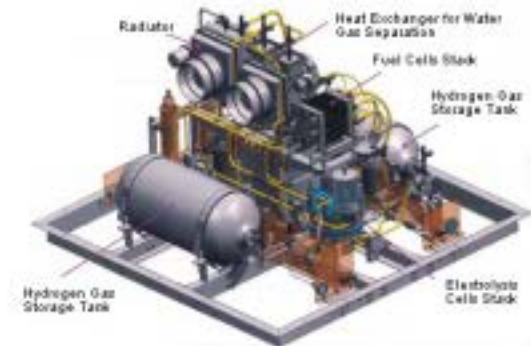


VRB (Prudent Energy) PacifiCorp (Moab, Utah) 2 MWh VRB-ESS

Source: <http://www.pdenenergy.com/>

Regenerative fuel cells

- Gaseous electrode materials
- Emerging technologies (H₂-O₂ conventional and unitized)
- New chemistries (H₂-Br₂, H₂-H₂O₂, NaBH₄-H₂O₂)

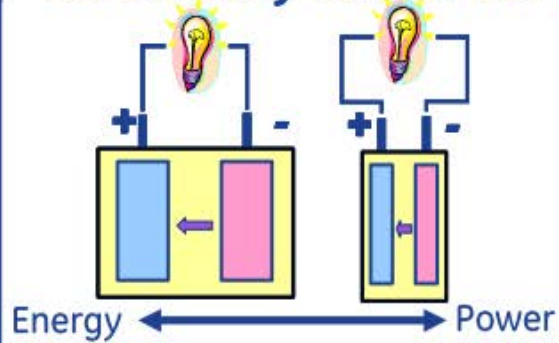


1kW-prototype Regenerative Fuel Cell System

Source: www.apg.jaxa.jp

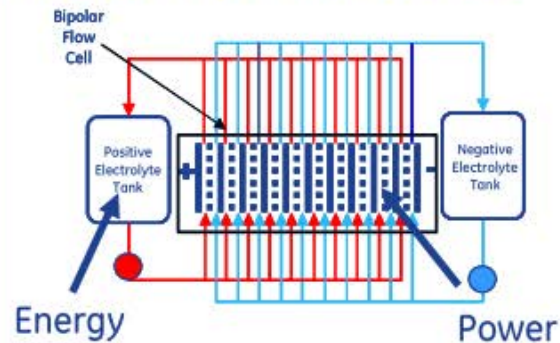
Electrochemical Energy Storage Comparison

Secondary batteries



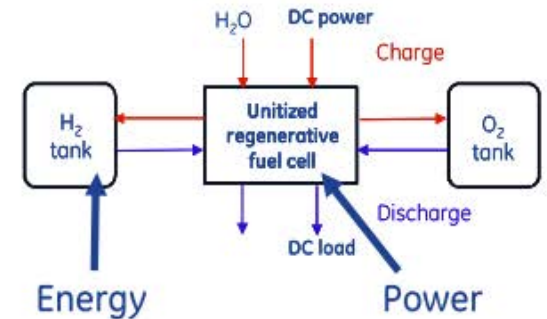
- No power-energy separation
- Moderate energy density (50 – 240 Wh/kg)
- High energy efficiency (65 – 90 %)
- Degradation mode – electrode
- Linear scalability (small cells)
- Moderate cost
- Mature technology

Redox flow batteries



- Power and energy separated
- Low energy density (10 – 50 Wh/kg)
- High energy efficiency (65 – 78 %)
- Degradation mode – membrane
- Non-linear scalability (cell stacks)
- Low cost
- Emerging technology

Regenerative fuel cells



- Power and energy separated
- High energy density (450 – 500 Wh/kg)
- Low energy efficiency (35 – 50 %)
- Degradation mode – catalyst
- Non-linear scalability (cell stacks)
- High cost
- New technology

Unitized Regenerative Fuel Cell (URFC)

Desired for applications that require high energy density and low weight

- Cars
- Solar powered aircraft
- Micro-spacecraft
- Load-leveling for wind turbines and Solar Cells

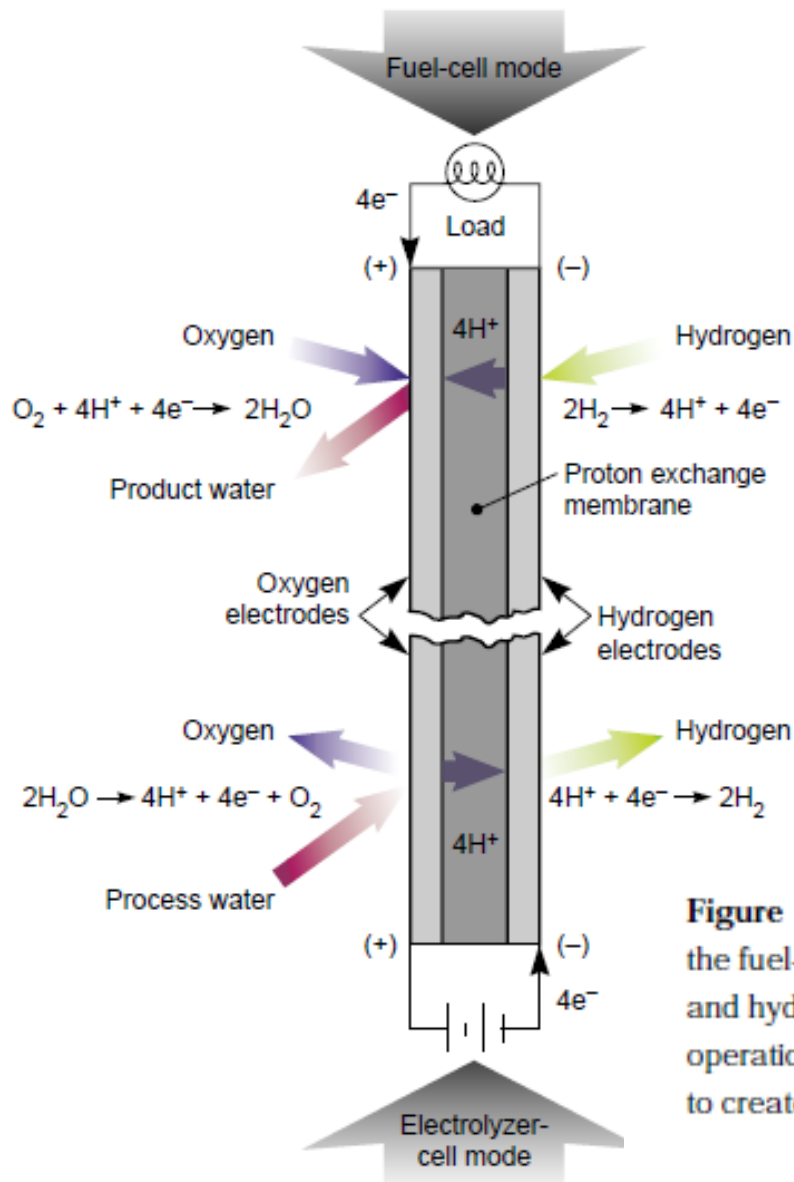
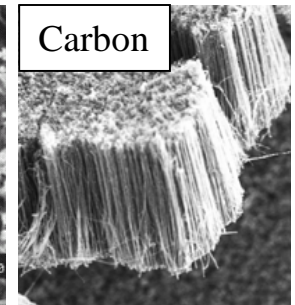
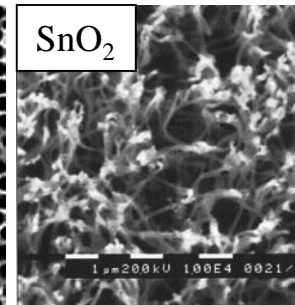
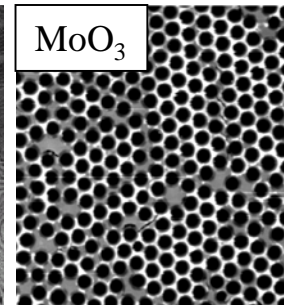
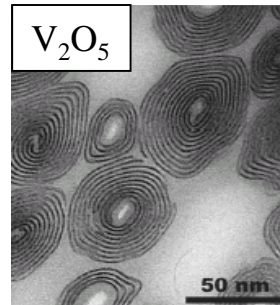


Figure 1. The electrochemistry of a unitized regenerative fuel cell. In the fuel-cell mode, a proton-exchange membrane combines oxygen and hydrogen to create electricity and water. When the cell reverses operation to act as an electrolyzer, electricity and water are combined to create oxygen and hydrogen.

Tailoring of Nanostructured Materials

Purposeful Tailoring of Structure, Shape, Composition, Orientation

Desired Attributes
High Surface Area 10-1000 m²/g
High Porosity 50-97 %
Low Density 0.005-2 g/cm³



Templating & Structure Directing Agents

Catalyst particles (Iron, Cobalt, Gold)

Leiber, Smalley

Surfactants (alkylamines, block co-polymers)

Nesper, Turner

Membranes (Al₂O₃, polycarbonate,)

Martin, Caruso

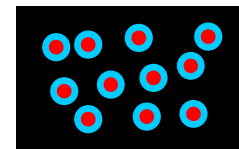
Colloidal-crystals (latex, PS, SiO₂)

Stein, Bartlett, Dunn

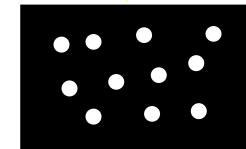
Macromolecular (dendrimers)

Crooks, Chandler

● Templating agent

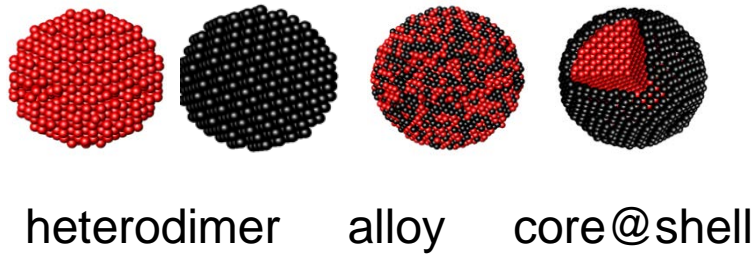


↓
Template Removal

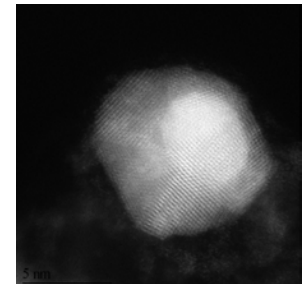
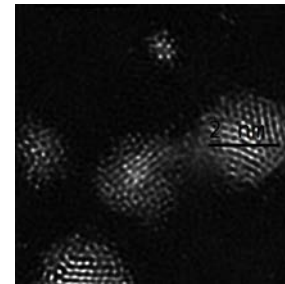
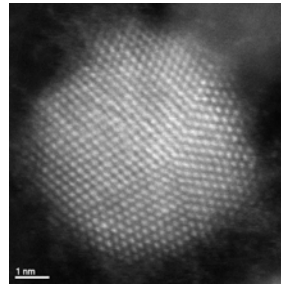


New Materials with Uncharacterized Structure/Property Relationships

Catalyst Architectures

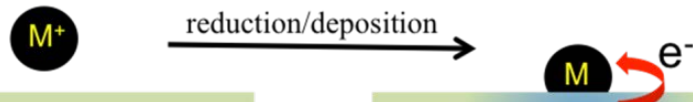


PtCu, PdCu, PdAg, PtPd, PdIr, PdMo

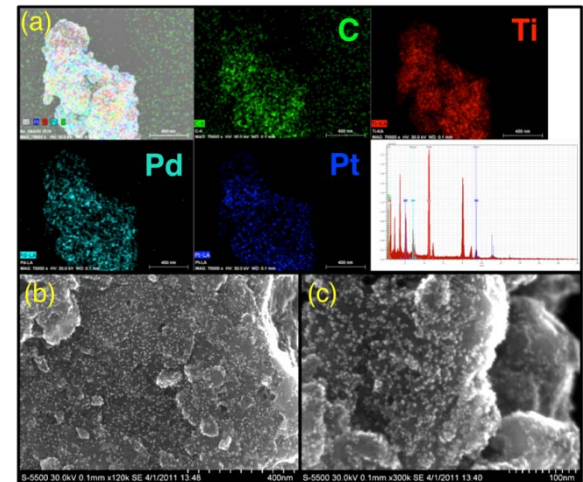
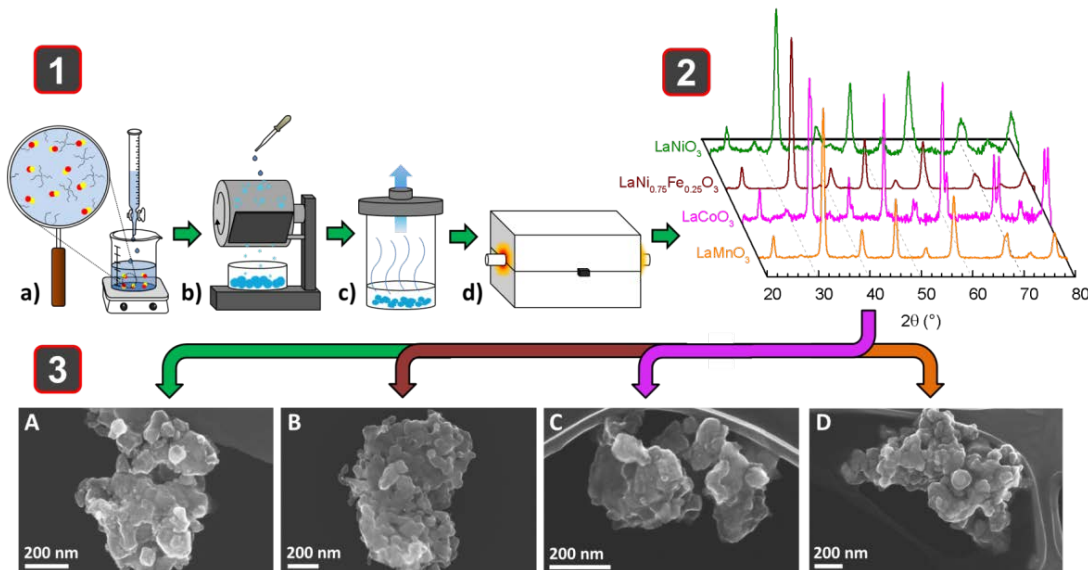


JACS **2012**, 134(23), 9812

J. Phys. Chem. C. **2012**, 116(20), 11032



TiO₂(b), MnO₂, LaMO₃, MoS₂, Fe₃O₄



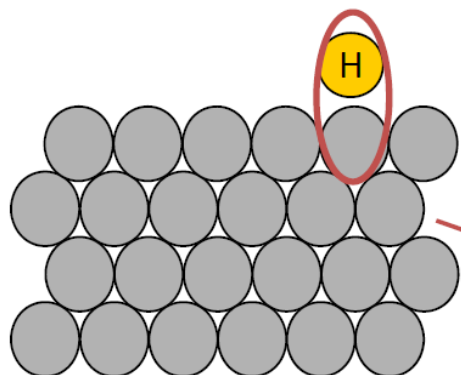
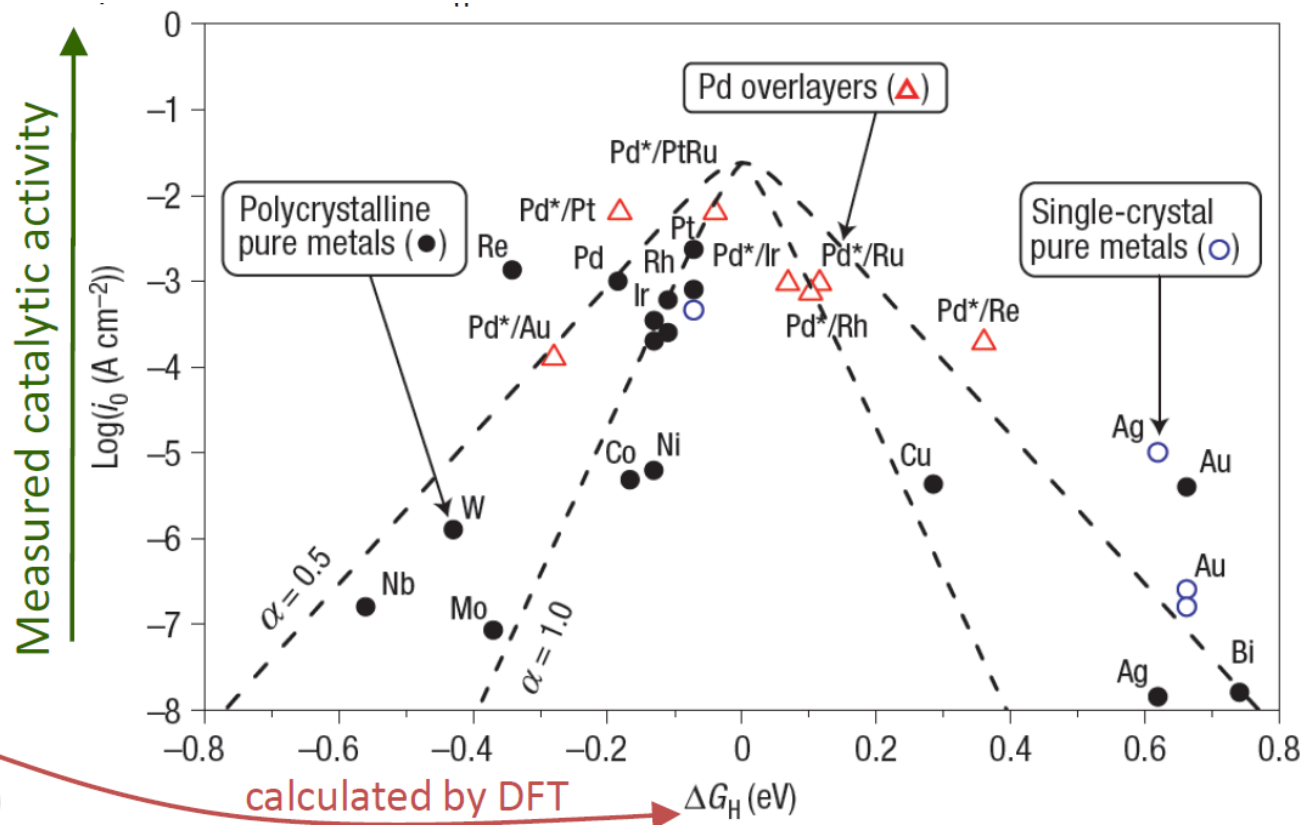
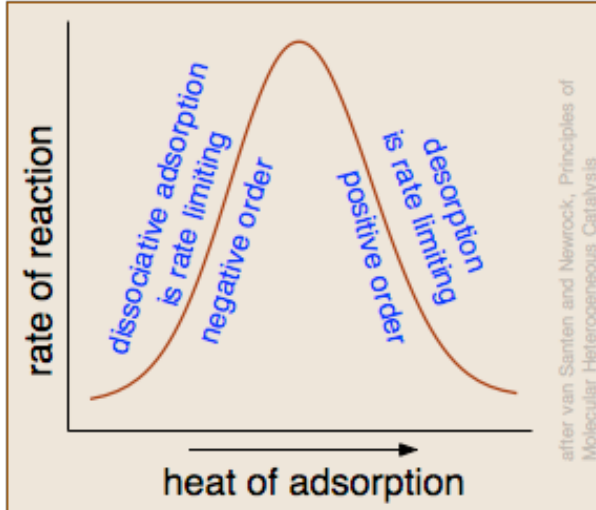
Chem. Commun. **2011**, 47(44), 12104

J. Phys. Chem. Lett. **2013**, 4, 1254

J. Mater. Chem. A **2013**, 1, 13443

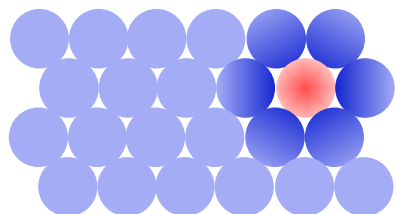
Chem. Mater. **2014**, 26, 3368

Activity Descriptors for Catalysis



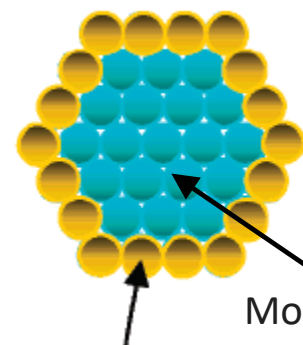
Activity Enhancement Effects from Catalysts

Ligand Effects



→ *Electron donation from dissimilar surface atoms*

Geometric Effects



→ *Specific atomic arrangement of surface atoms*

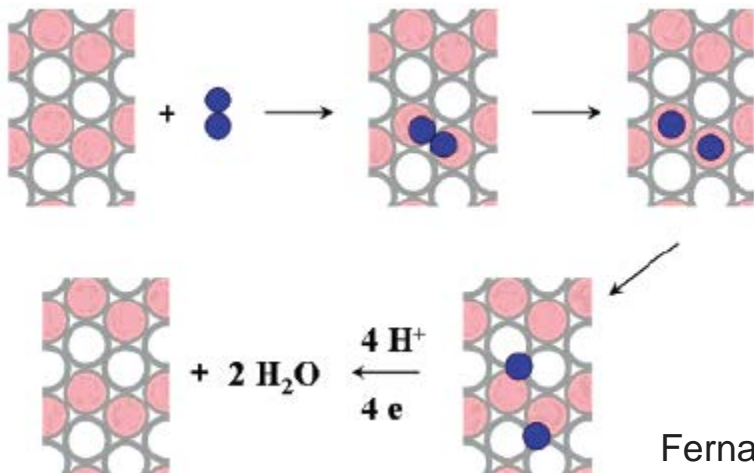
Strained monolayer shell

Monometallic core

J. Zhang. *J. Phys. Chem. B.* 2005.

Modify the binding energy of reaction intermediates

Ensemble Effects



→ Different atomic sites or clusters *cooperate to facilitate distinct reaction steps*

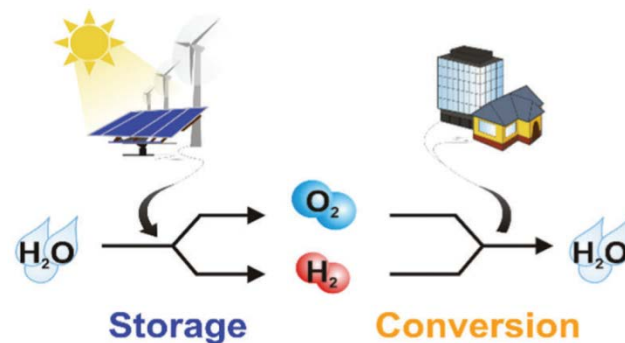
e.g. oxygen bond cleaving vs formation and desorption of water

Fernandez, Walsh & Bard *J. Am. Chem. Soc.* 2005.

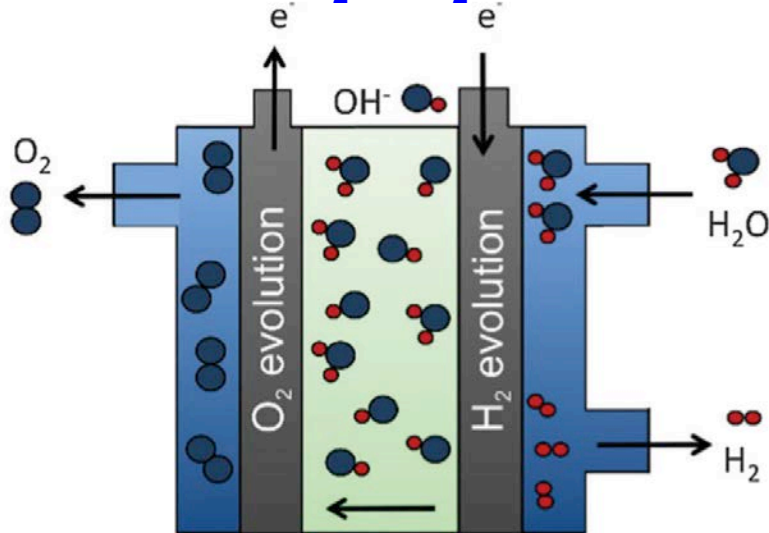
Oxygen Electrochemistry

Oxygen Chemistry is Ubiquitous

- Electrolyzers for H₂ generation
- Metal-air batteries (Zn-air, Li-air)

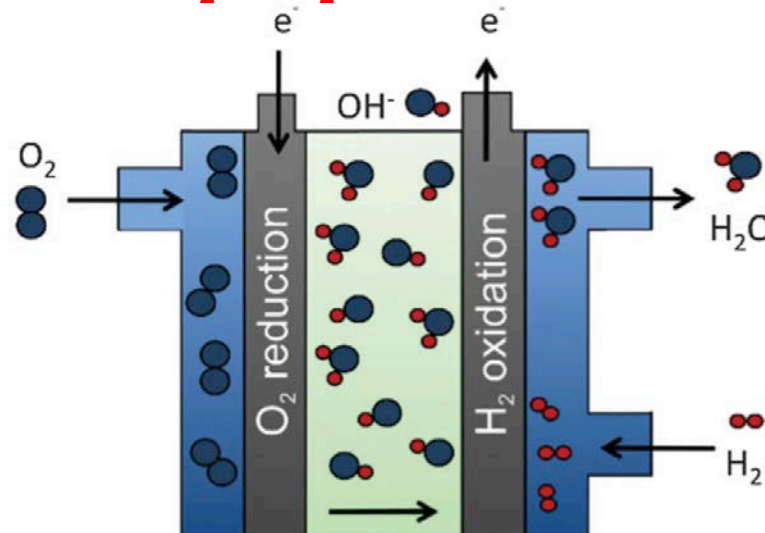


oxygen evolution reaction (OER)



Electrolyzer

oxygen reduction reaction (ORR)

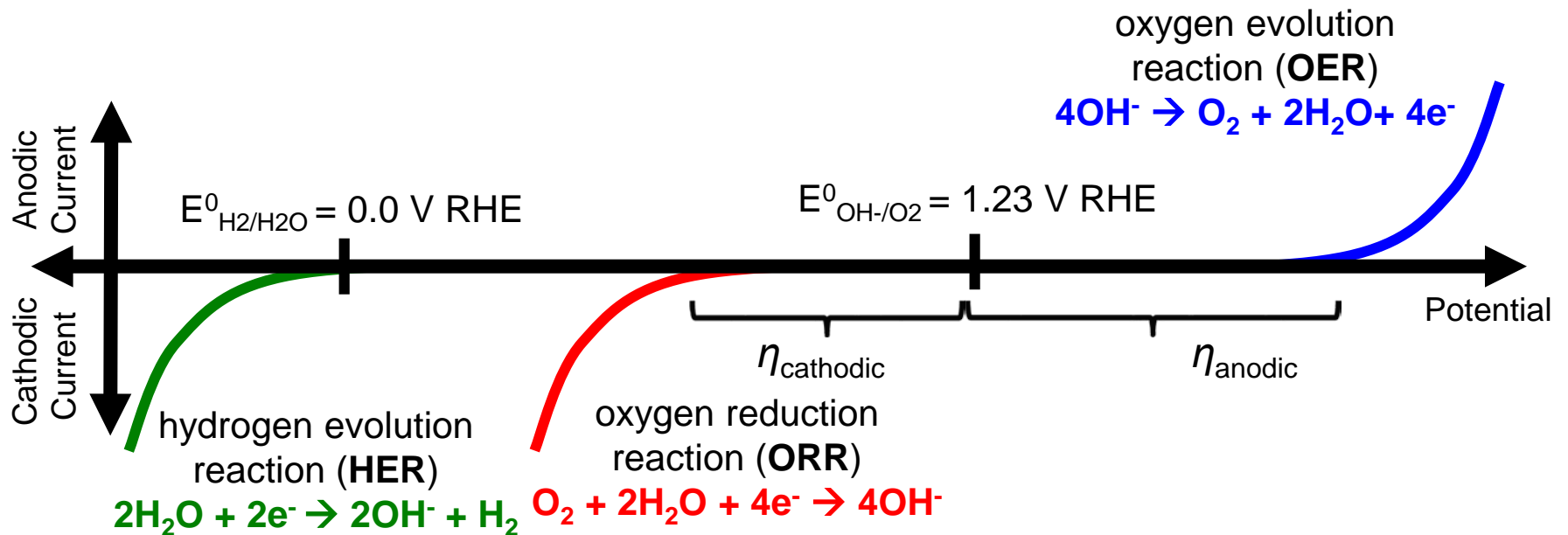


Fuel Cell

OER and ORR

Thermodynamics vs Kinetics

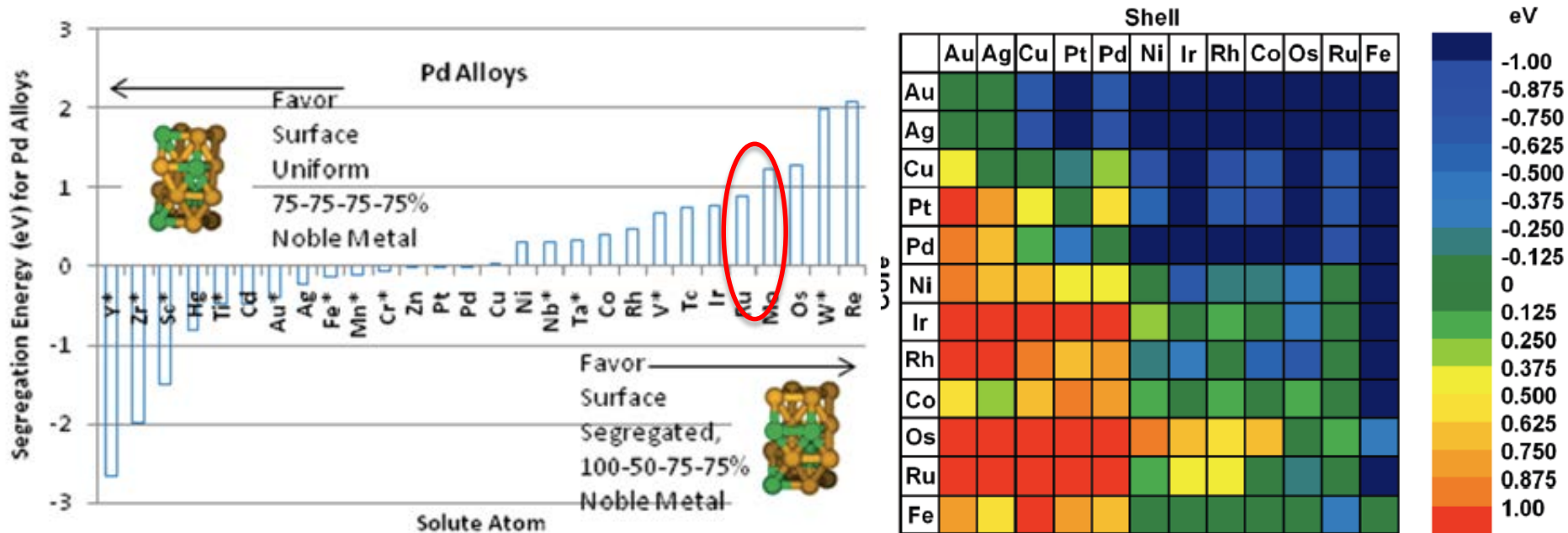
- “kinetically sluggish” reactions require large overpotentials ($\eta \geq 300$ mV)
- Large overpotentials result in lower power, device efficiency



Catalyst materials

- Materials capable of both OER and ORR for regenerative fuel cells → ‘bifunctional’ catalysts
- Alkaline electrolyte enables non-precious metal oxides → Perovskites

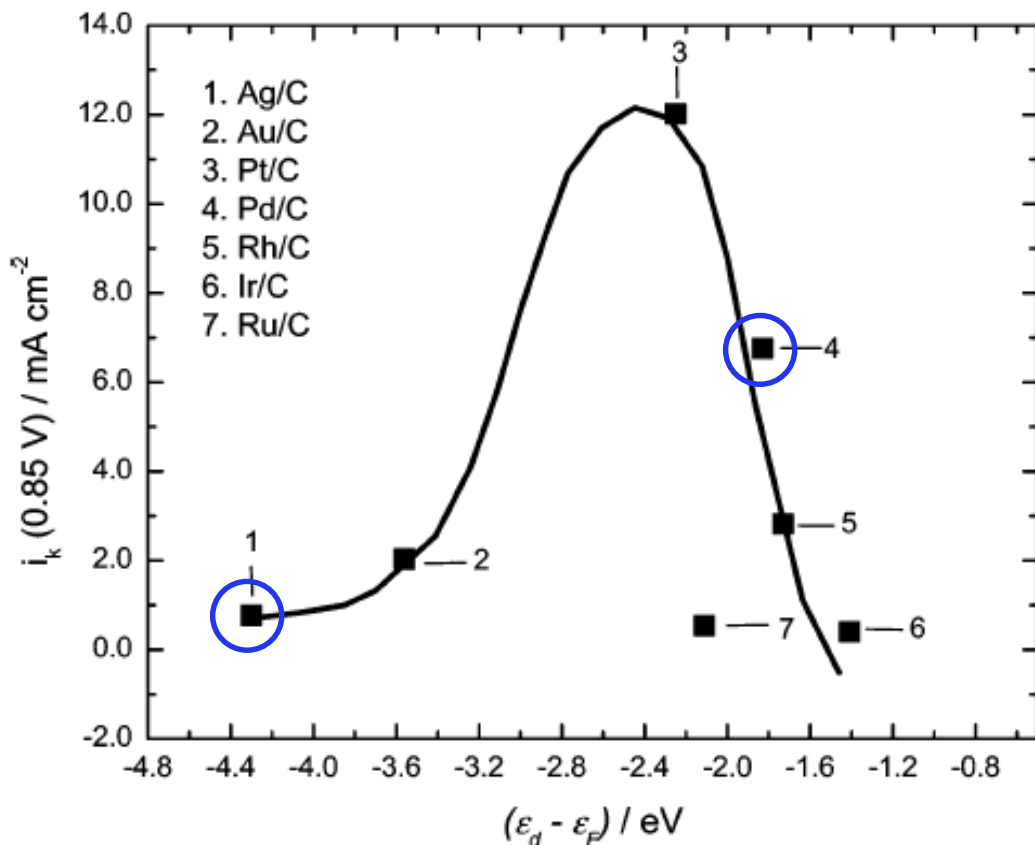
“Predictions” on Synthesis of Pd Alloy & Core@Shell Catalysts



Calculations predict stability of Ir, Ru, Mo, W, Re@Pd core@shell structure And homogeneous alloy formation for PdAg & PdAu.

Rationale for Choosing Pd-Ag Alloy

Volcano Dependence of Activity on DFT Calculated d-band Centers



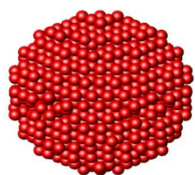
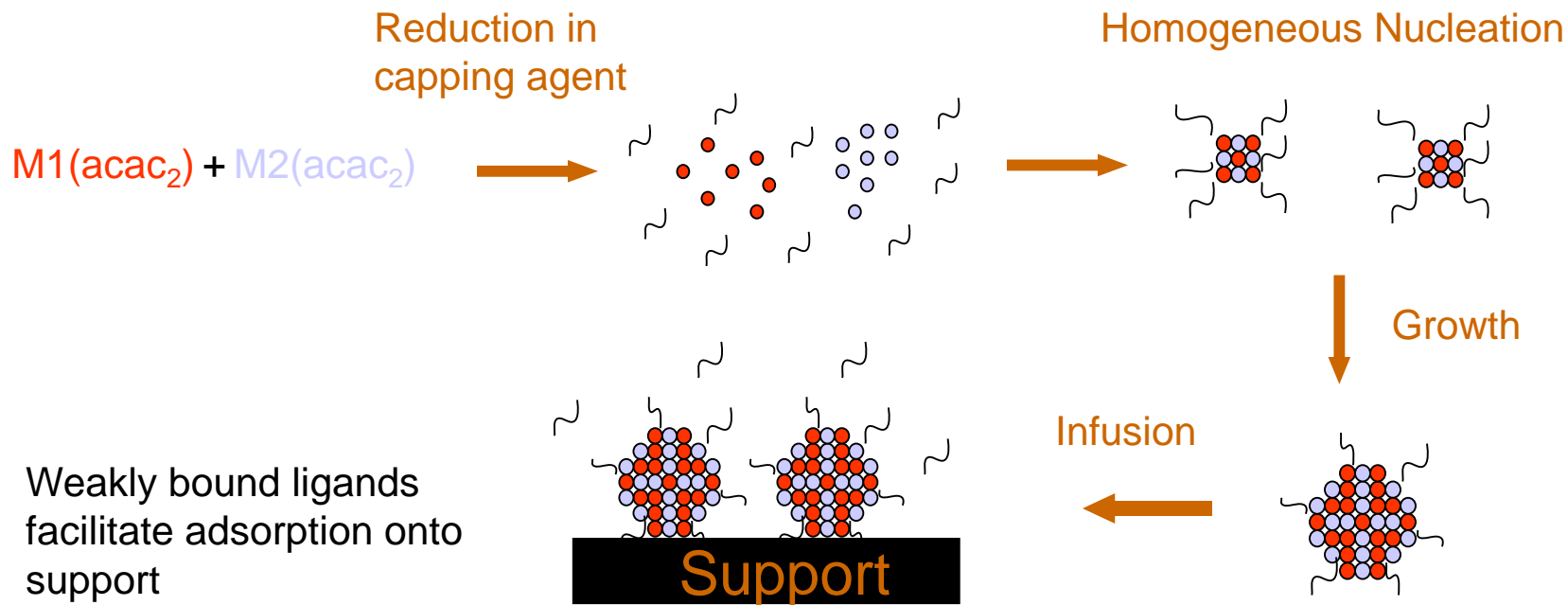
Ensemble Effect: Oxygen Binding on Ag is too weak, whereas too strong on Pd

Economics: Pd (\$630/troy oz) vs Ag (\$30/troy oz)

Both Ag and Pd FCC metals → form solid solutions over compositional range

Challenge: Controlled synthesis of uniform alloys to take advantage of potential Pd-Ag synergy

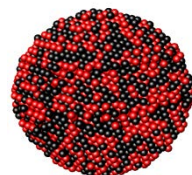
Synthesis of Catalyst Architectures



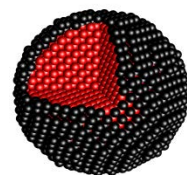
heterodimer



alloy



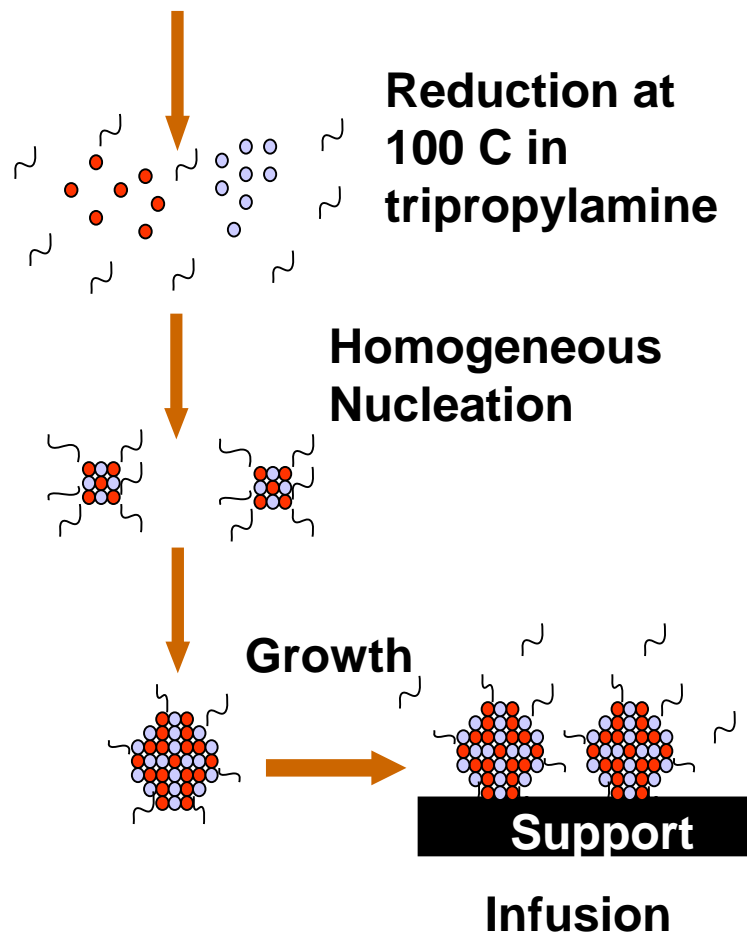
core@shell



How does size, shape, composition and morphology influence properties?

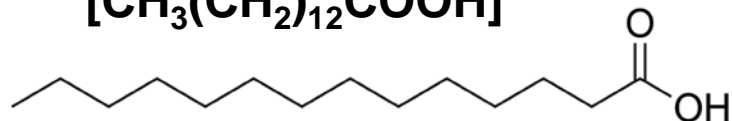
Synthesis of Ag-Rich Ag-Pd Alloy Catalysts

Pd(II)-TDOA + Ag-TDOA



Tetradecanoic acid

$[\text{CH}_3(\text{CH}_2)_{12}\text{COOH}]$

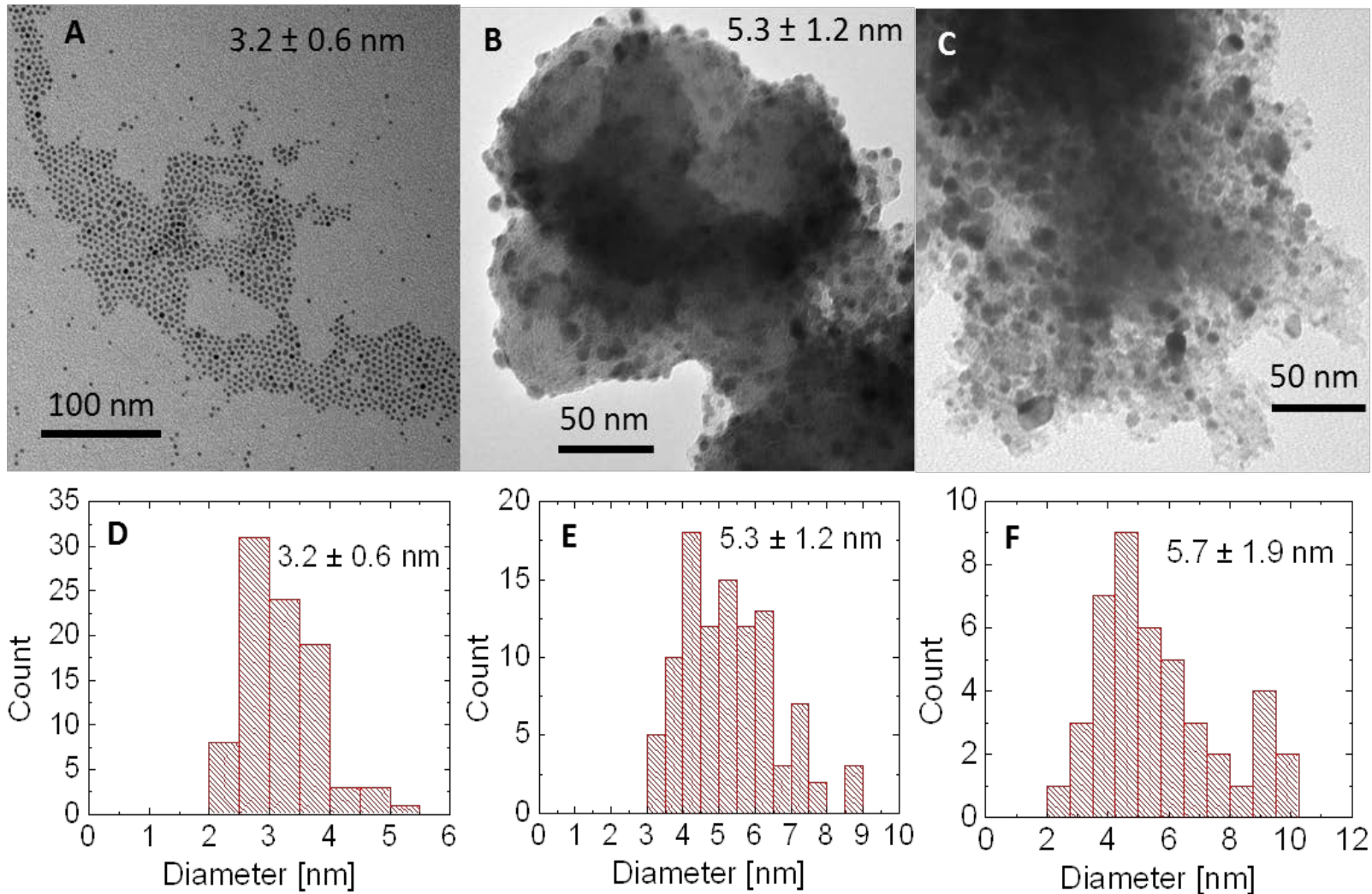


Ratio of Ag & Pd determines final alloy stoichiometry. Metal concentration always fixed at 1 mmol, theoretical reaction yield of ~105 mg.

- Slow ramp to 100C, hold for 1 hr.
- React under Ar / N₂.
- Forms kinetic alloy
- Close to 100% yield

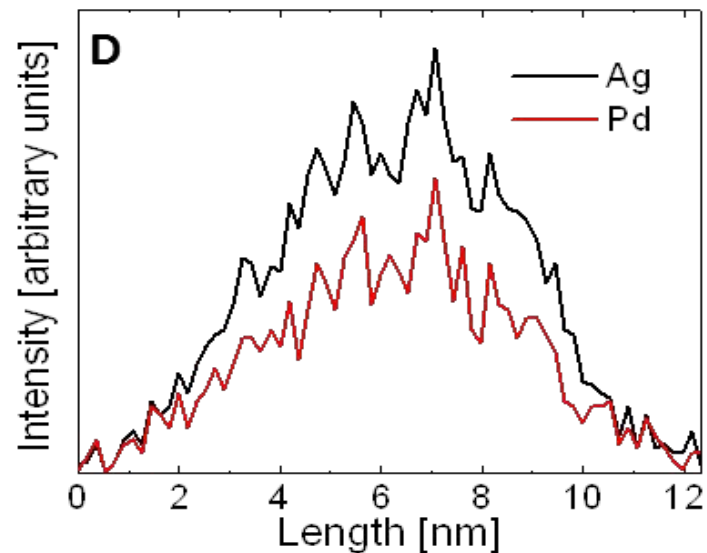
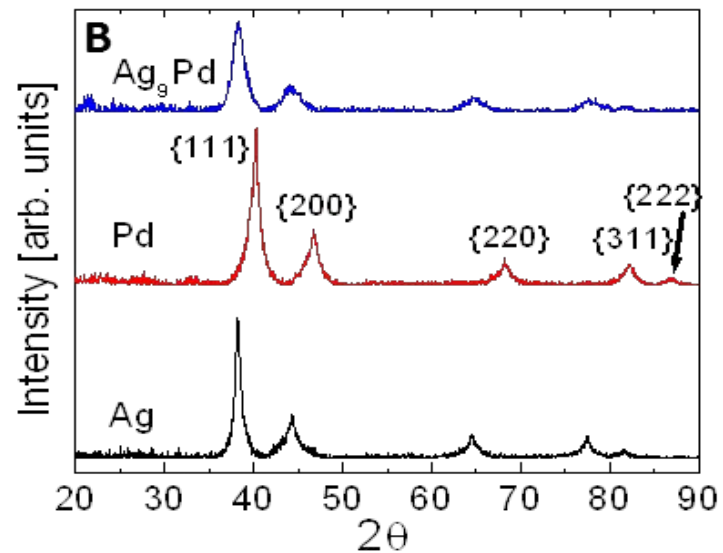
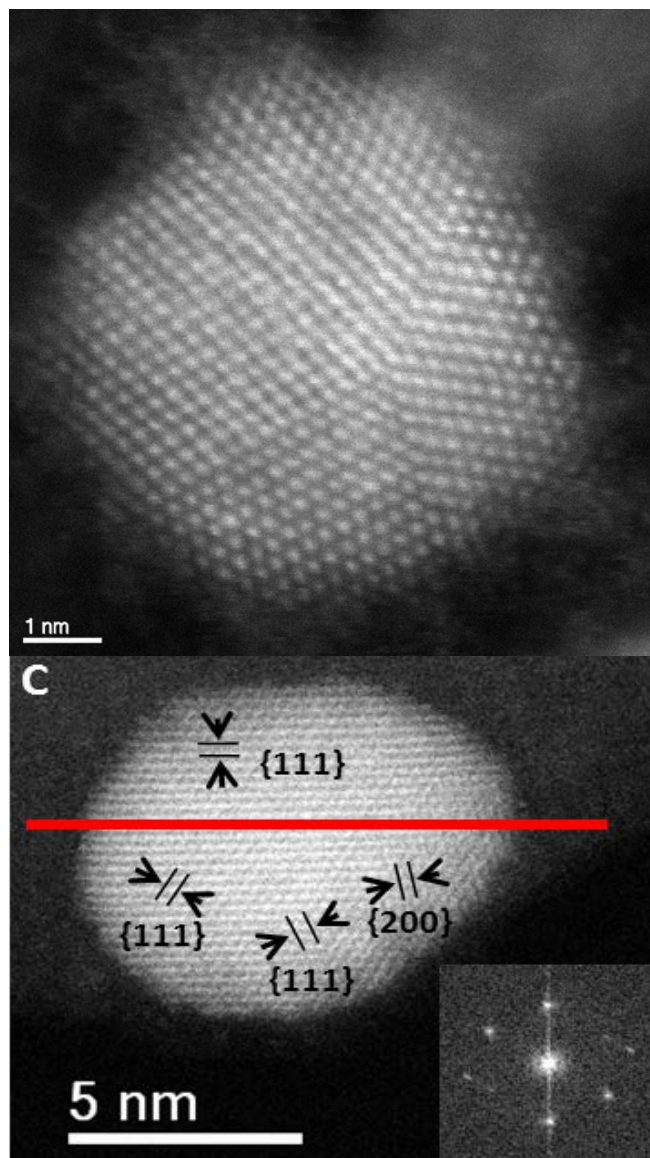
Particles are 30% (by weight) ligand, results in ~130 mg yield per reaction.

Homogeneous Ag-Pd Nanoalloys



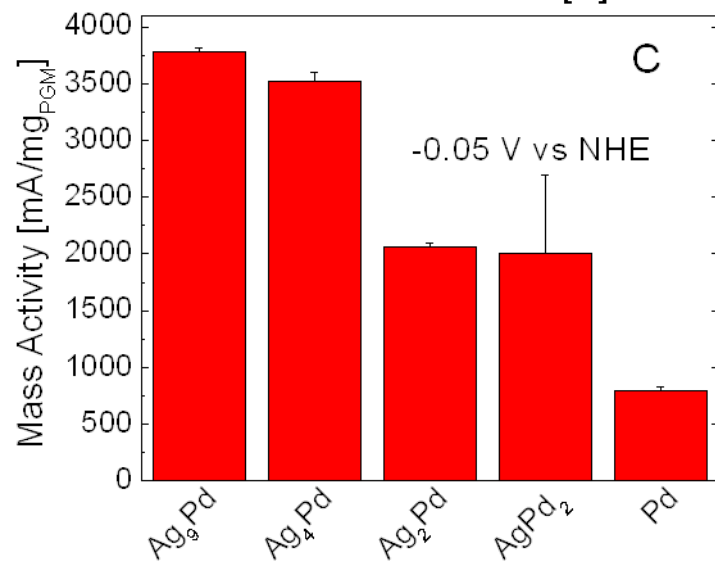
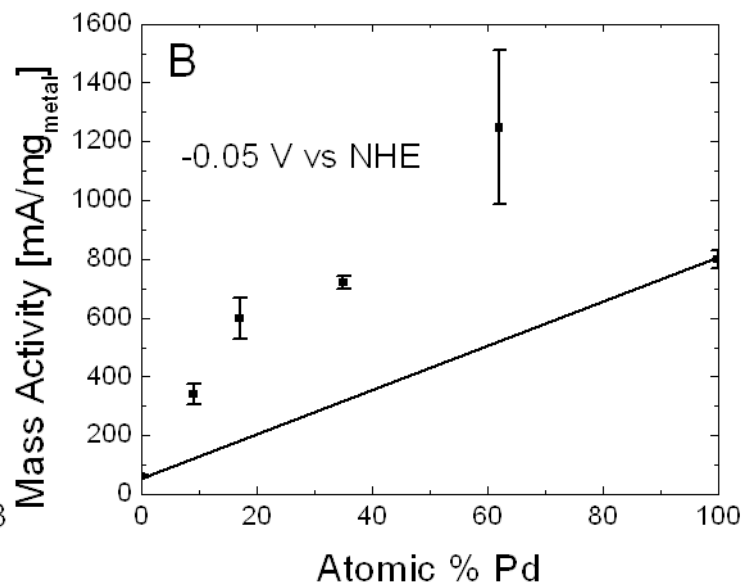
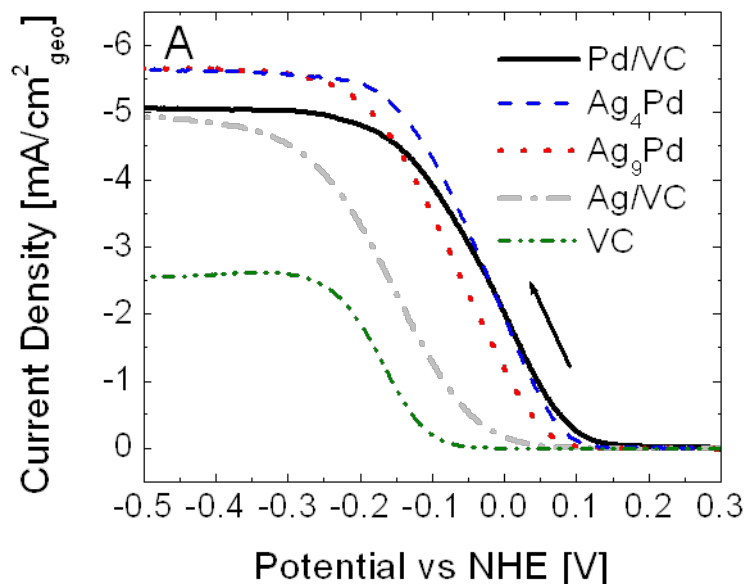
(A) as-synthesized Ag₉Pd nanoparticles, (B) Vulcan XC72 carbon supported Ag₉Pd particles after calcination at 450°C in N₂, and (C) commercial Pd/VC calcined at 450°C N₂. The alloy particles undergo slight sintering from 3.2 to 5.3 nm.

Homogeneous Ag-Pd Nanoalloys



D. Slanac et al. *JACS* 2012.

Activity Synergy from Ensemble and Ligand Effects



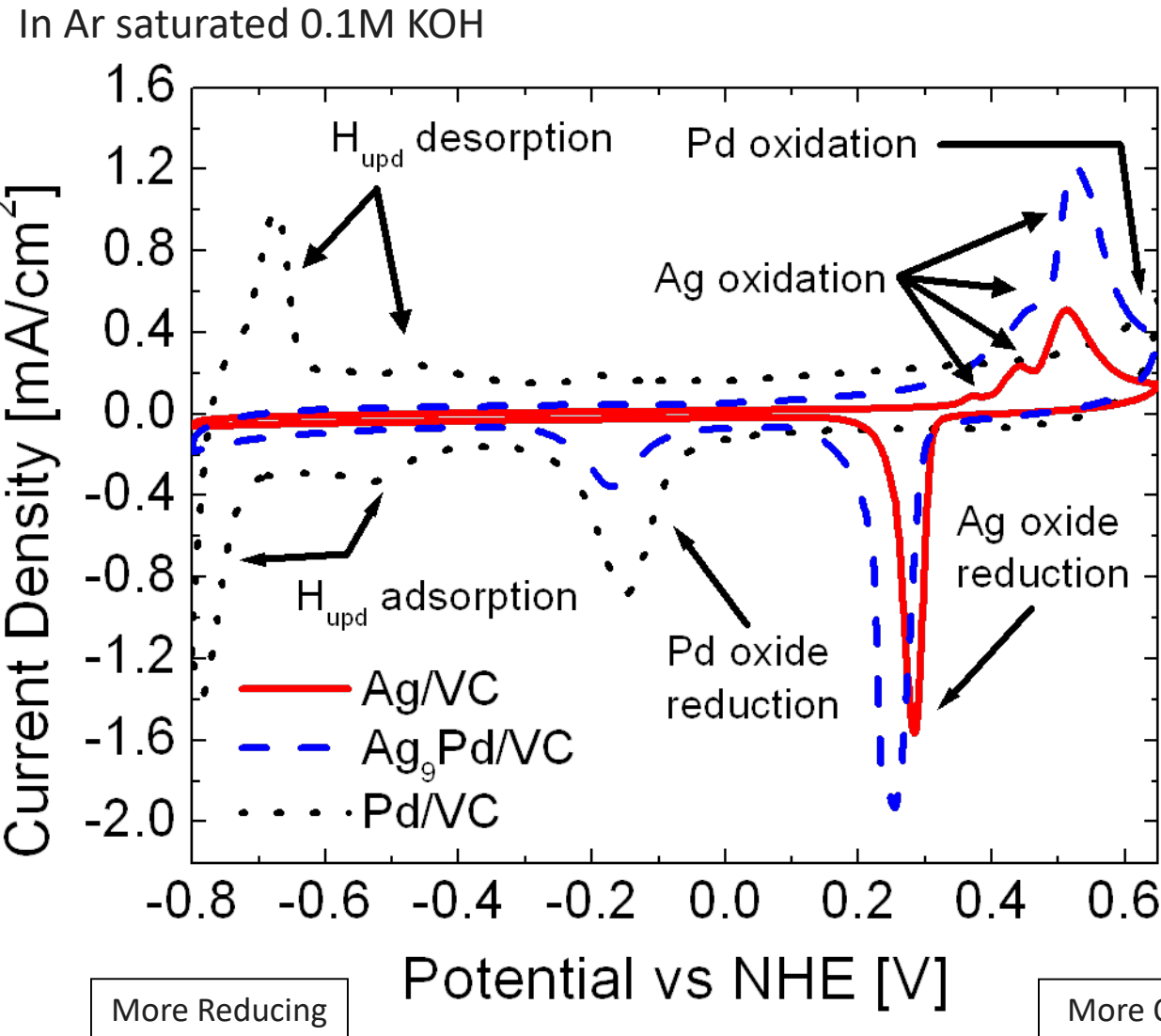
Total mass activity up to 4x over the expected linear combination of Ag and Pd

**Pd helps O₂ bond breaking
Ag facilitates desorption of OH⁻**

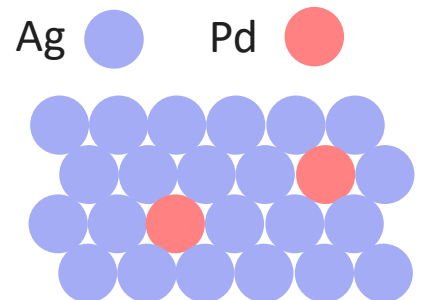
Per expensive Pd metal, ~4x activity enhancement

Atomic % Pd

Electrochemical Evidence of Pd Single Atoms



1. Both Pd and Ag present in surface (reduction peaks)
2. No H_{upd} on alloy surface
3. Minimum of Pd dimers to give H_{upd}
4. Shift in metal ox/red peaks → ligand effect
5. Pd facilitates oxygen, binding, and Ag facilitates desorption

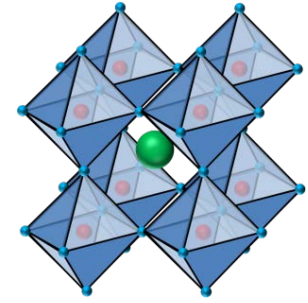


What is a Perovskite?

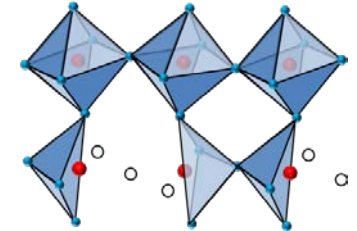
hydrogen 1 H 1.0079																	helium 2 He 4.0026	
lithium 3 Li 6.941	beryllium 4 Be 9.0122																	neon 10 Ne 20.180
sodium 11 Na 22.990	magnesium 12 Mg 24.305																	argon 18 Ar 39.948
potassium 19 K 39.098	calcium 20 Ca 40.078	scandium 21 Sc 44.956	titanium 22 Ti 47.887	vanadium 23 V 50.942	chromium 24 Cr 51.996	manganese 25 Mn 54.938	iron 26 Fe 55.845	cobalt 27 Co 58.933	nickel 28 Ni 58.693	copper 29 Cu 63.546	zinc 30 Zn 65.39	gallium 31 Ga 69.723	germanium 32 Ge 72.61	arsenic 33 As 74.922	selenium 34 Se 78.96	bromine 35 Br 79.904	krypton 36 Kr 83.80	
rubidium 37 Rb 85.468	strontium 38 Sr 87.62	yttrium 39 Y 88.906	zirconium 40 Zr 91.224	niobium 41 Nb 92.906	niobium 42 Mo 95.94	technetium 43 Tc [98]	ruthenium 44 Ru 101.07	rhodium 45 Rh 102.91	palladium 46 Pd 106.42	silver 47 Ag 107.87	cadmium 48 Cd 112.41	indium 49 In 114.82	tin 50 Sn 118.71	antimony 51 Sb 121.76	tellurium 52 Te 127.60	iodine 53 I 126.90	xenon 54 Xe 131.29	
cesium 55 Cs 132.91	barium 56 Ba 137.33	lanthanum 57 La 138.91	hafnium 72 Hf 178.49	tantalum 73 Ta 180.95	tungsten 74 W 183.84	rhenium 75 Re 186.21	osmium 76 Os 190.23	iridium 77 Ir 192.22	platinum 78 Pt 195.08	gold 79 Au 196.97	mercury 80 Hg 200.59	thallium 81 Tl 204.38	lead 82 Pb 207.2	bismuth 83 Bi 208.98	polonium 84 Po [209]	astatine 85 At [210]	radon 86 Rn [222]	
francium 87 Fr [223]	radium 88 Ra [226]	actinium 89 Ac [227]	actinide series	actinide series	actinide series	actinide series	actinide series	actinide series	actinide series	actinide series	actinide series	actinide series	actinide series	actinide series	actinide series	actinide series	actinide series	

■ A-site
■ B-site
■ C-site

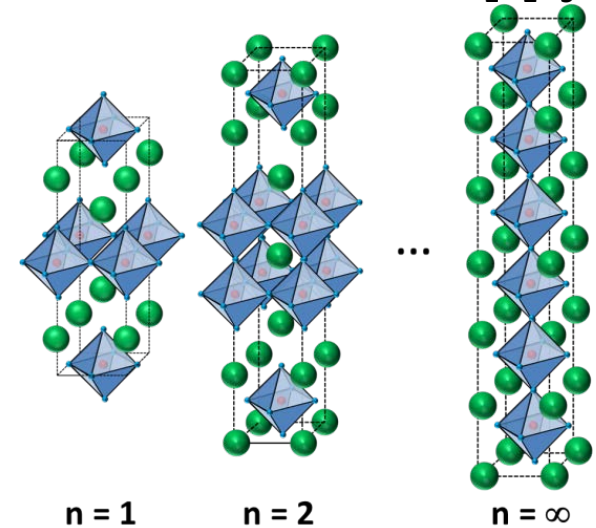
● A
● B
● C



Perovskite: ABC_3



Brownmillerite: $A_2B_2C_5$



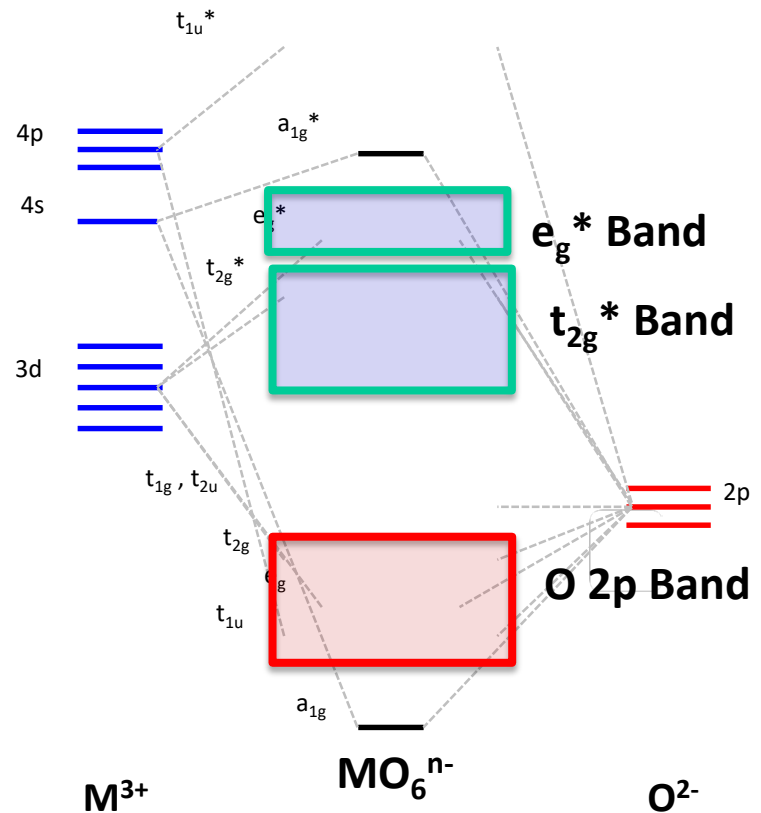
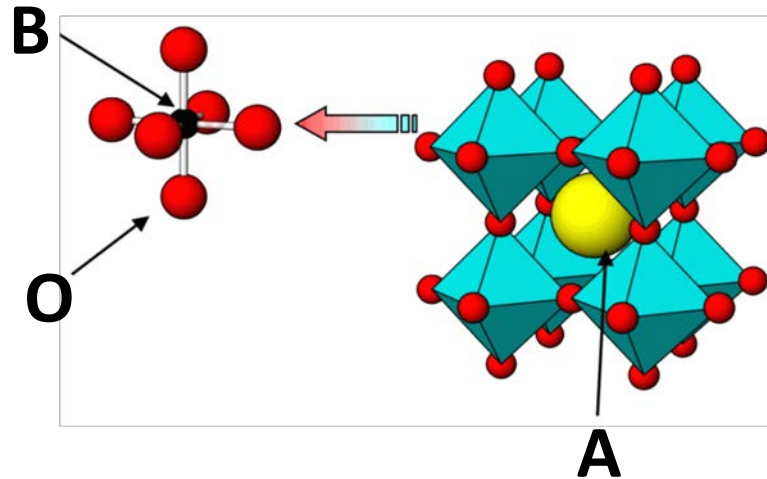
Ruddlesden-Popper: $(AC)(ABC_{3+\delta})_n$

- Simple Cubic with formula ABC_3
- Generally form at high temperatures ($>700^\circ C$), low S.A.
- Mixed ionic-electronic conductors
- Only B-Site is catalytically active

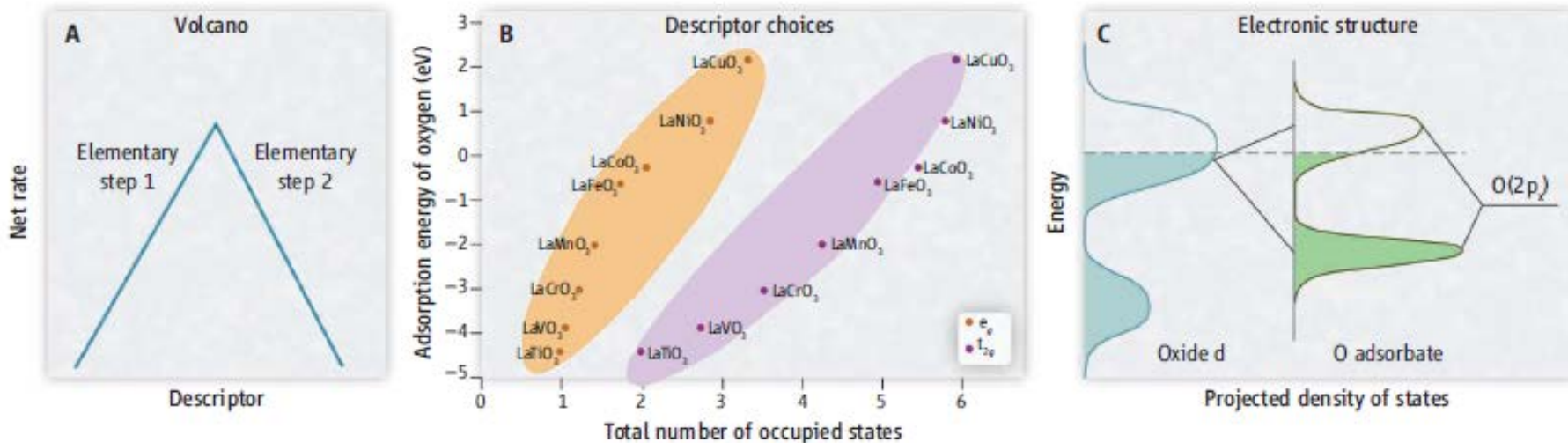
Background & Structure

Perovskite-type oxide ABO_3

- B-site atom (1st row transition metal) in 6-fold octahedral coordination
- BO_6 units breaks d manifold degeneracy
- Cubic, hexagonal \rightarrow rhombohedral crystal structure, influenced by:
 - ionic sizes
 - B $3d - O 2p$ interactions
 - J-T distortions



Theory Guided Predictive Activity Descriptors



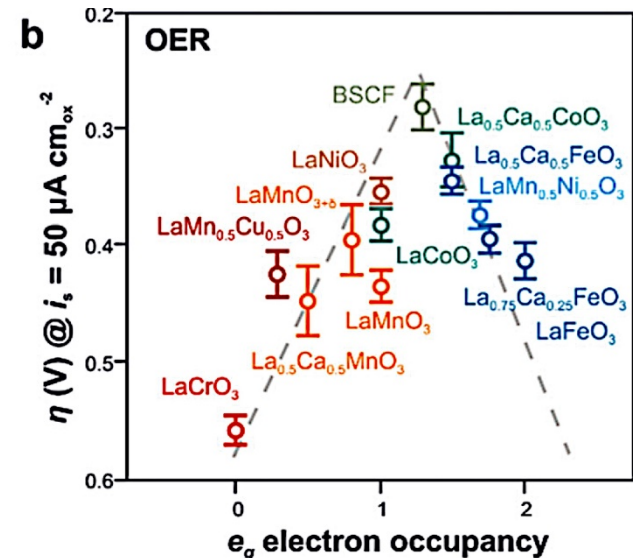
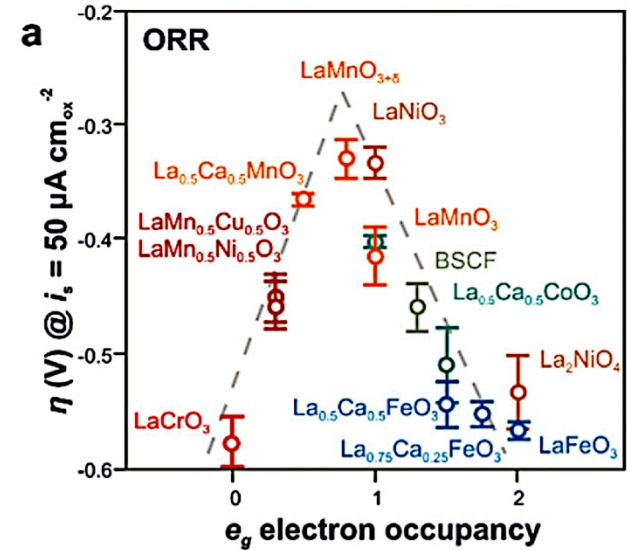
Optimizing Perovskites for the Water-Splitting Reaction
Aleksandra Vojvodic, *et al.*
Science 334, 1355 (2011);

Catalyst Design Principles

e_g filling of 1 proposed as governing descriptor of OER/ORR activity – Sabatier principle

- Filling >1 \rightarrow more antibonding \rightarrow OH^- too weakly bound
- Filling <1 \rightarrow more bonding \rightarrow OH^- too strongly bound

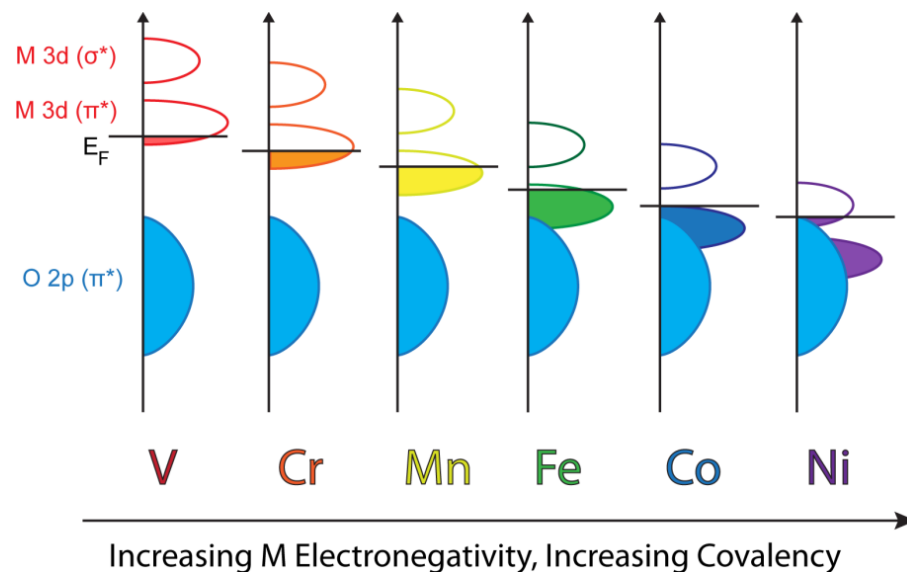
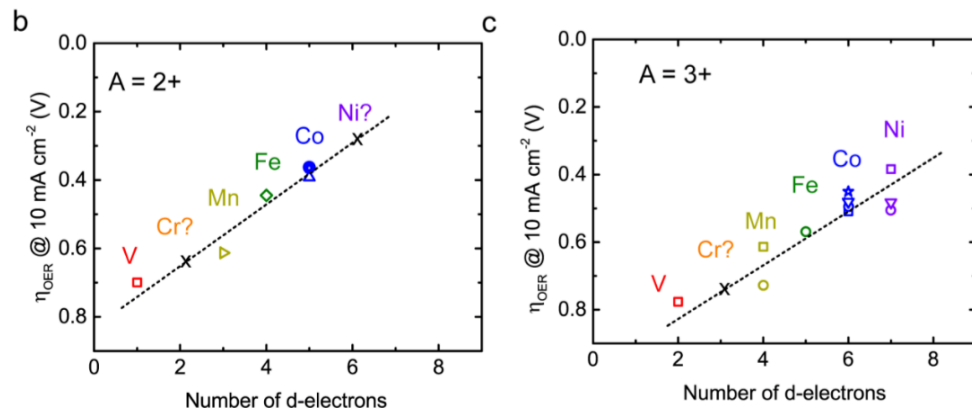
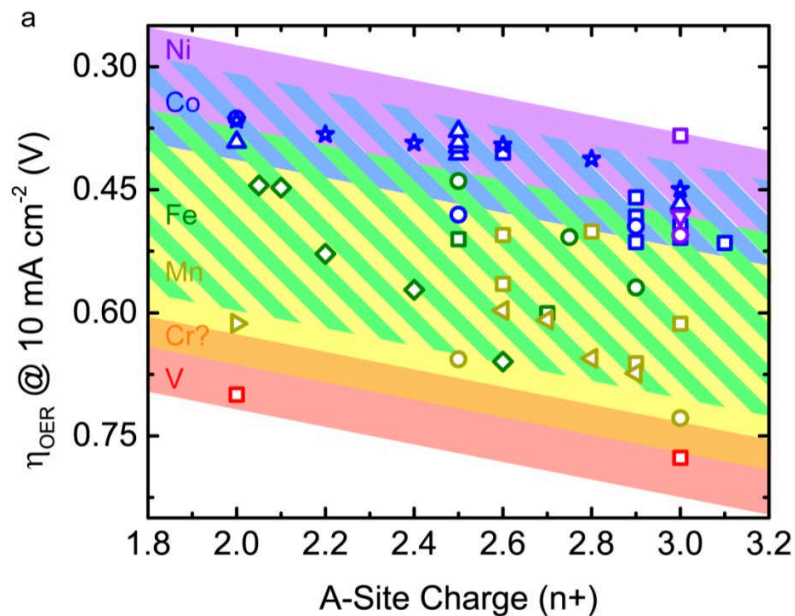
	$\text{Cr}^{3+} (d^3)$	$\text{Mn}^{3+} (d^4)$	$\text{Fe}^{3+} (d^5)$	$\text{Co}^{3+} (d^6)$	$\text{Ni}^{3+} (d^7)$
High Spin		e_g \uparrow $_$ t_{2g} \uparrow \uparrow \uparrow	e_g \uparrow \uparrow t_{2g} \uparrow \uparrow \uparrow	e_g \uparrow \uparrow t_{2g} $\uparrow\downarrow$ \uparrow \uparrow	e_g \uparrow \uparrow t_{2g} $\uparrow\downarrow$ $\uparrow\downarrow$ \uparrow
Intermediate Spin				e_g \uparrow $_$ t_{2g} $\uparrow\downarrow$ $\uparrow\downarrow$ \uparrow	
Low Spin	e_g $_$ $_$ t_{2g} \uparrow \uparrow \uparrow	e_g $_$ $_$ t_{2g} $\uparrow\downarrow$ \uparrow \uparrow	e_g $_$ $_$ t_{2g} $\uparrow\downarrow$ $\uparrow\downarrow$ \uparrow	e_g $_$ $_$ t_{2g} $\uparrow\downarrow$ $\uparrow\downarrow$ $\uparrow\downarrow$	e_g \uparrow $_$ t_{2g} $\uparrow\downarrow$ $\uparrow\downarrow$ $\uparrow\downarrow$



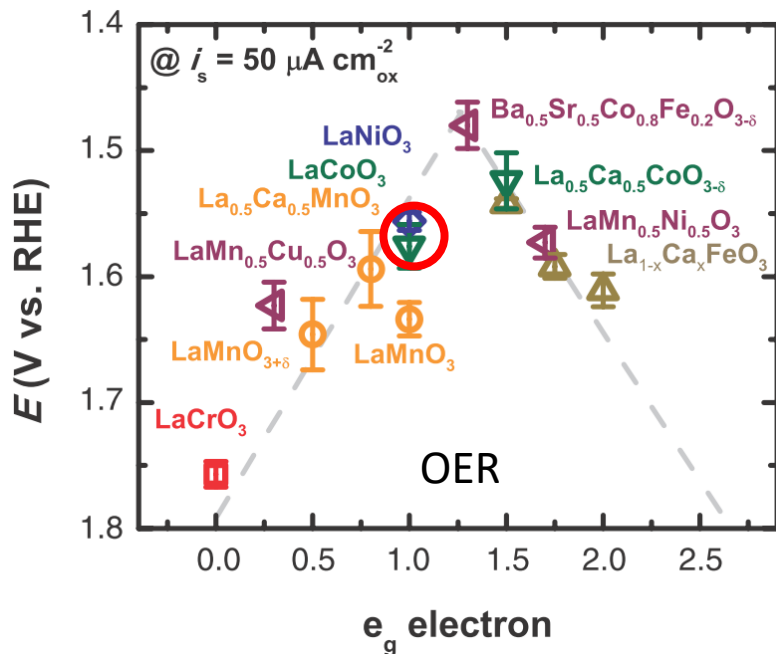
Catalyst Design Principles

More d electrons \rightarrow greater activity

- More electronegative TM brings 3d electron energies down
- More covalent M – O bond



Perovskite // Activity Relationships



e_g filling as catalytic descriptor

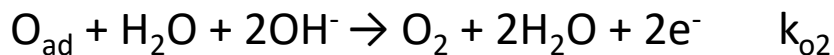
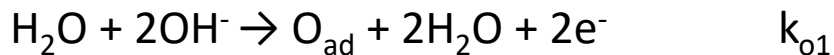
- same filling, different activity
- verify trend / reduce error

‘Covalency’ between M-O

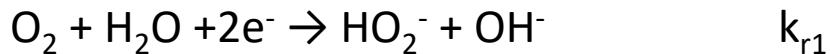
Catalyze $k_{o/r1}$, $k_{o/r2}$ or k_d



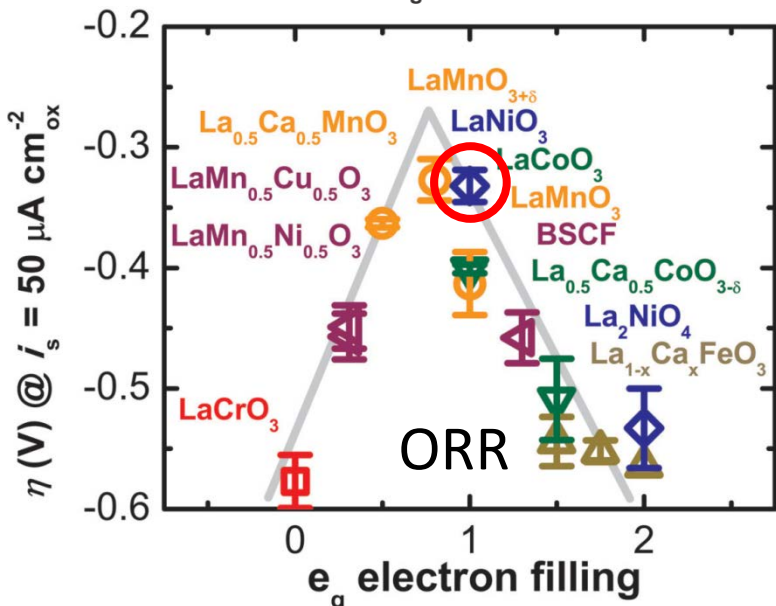
OER



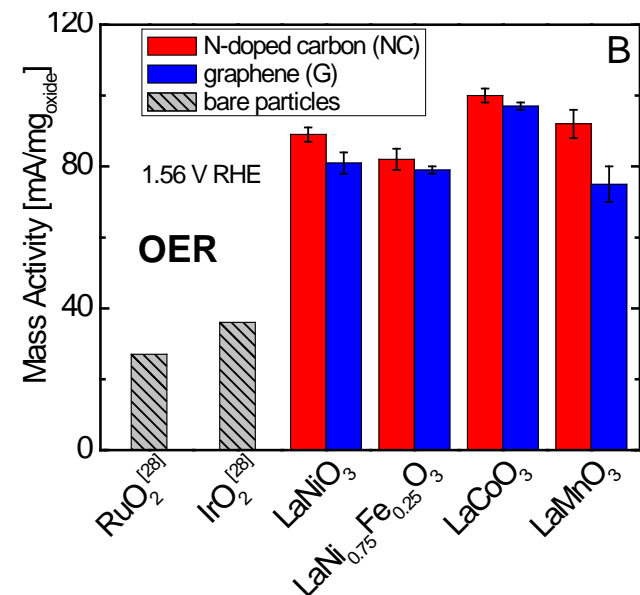
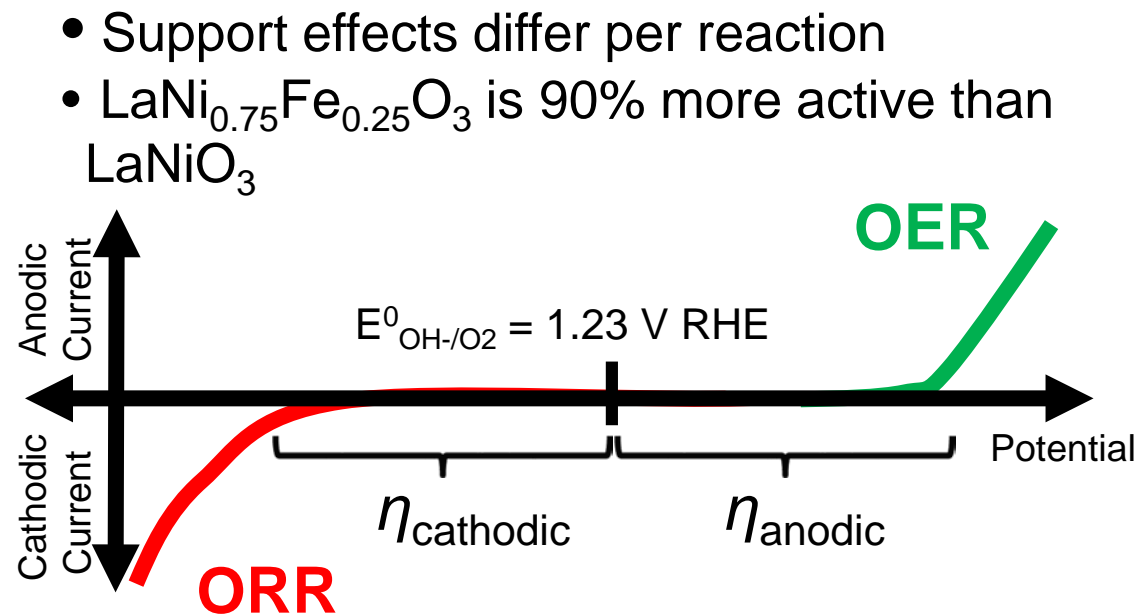
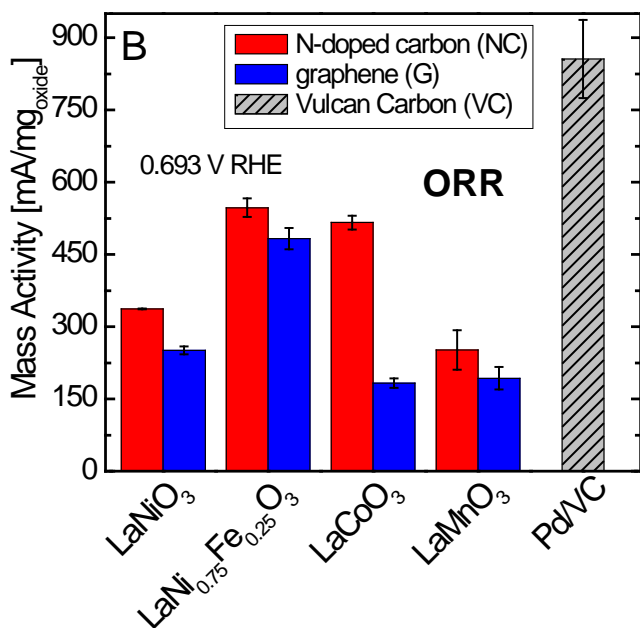
ORR



Chemical Disproportionation

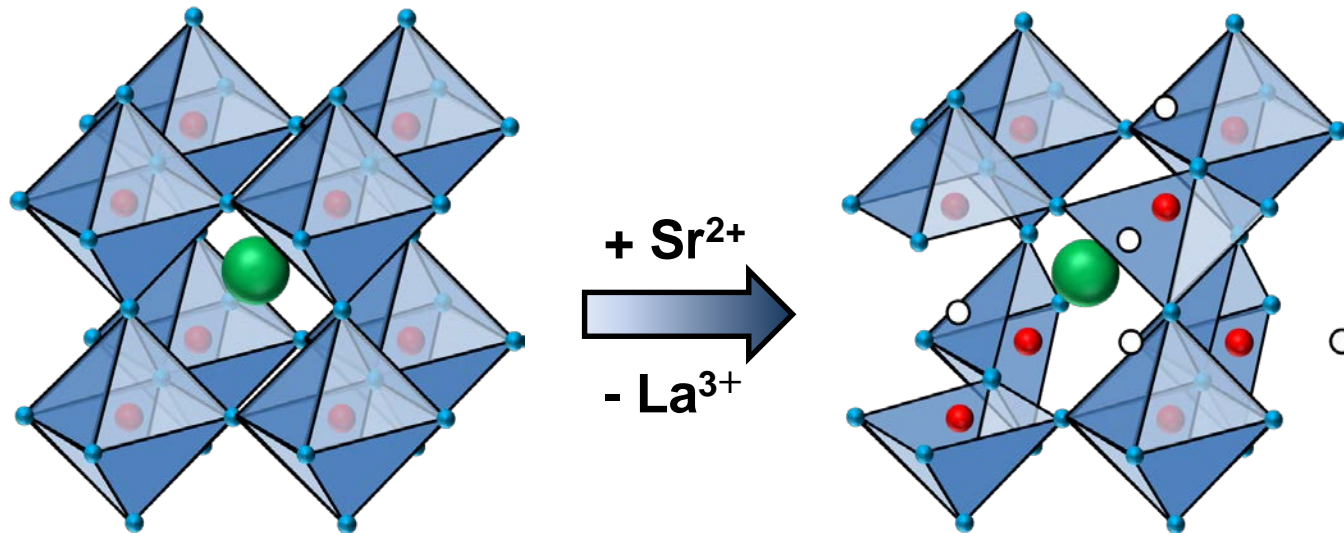


Bifunctional Perovskite Catalysts



Material	ORR Potential (V) vs RHE @ $j = -3 \text{ mA/cm}^2$	OER Potential (V) vs RHE @ $j = 10 \text{ mA/cm}^2$	ΔE (V) Bifunctionality
LaNiO ₃ /NC	0.64	1.66	1.02
LaNi _{0.75} Fe _{0.25} O ₃ /NC	0.67	1.68	1.01
LaCoO ₃ /NC	0.64	1.64	1.00
20% Ir/C [‡]	0.69	1.61	0.92
20% Ru/C [‡]	0.73	1.62	1.01
20% Pt/C [‡]	0.86	2.02	1.16

Using Chemical Substitution to Control Oxygen Content in $\text{La}_{1-x}\text{Sr}_x\text{CoO}_{3-\delta}$



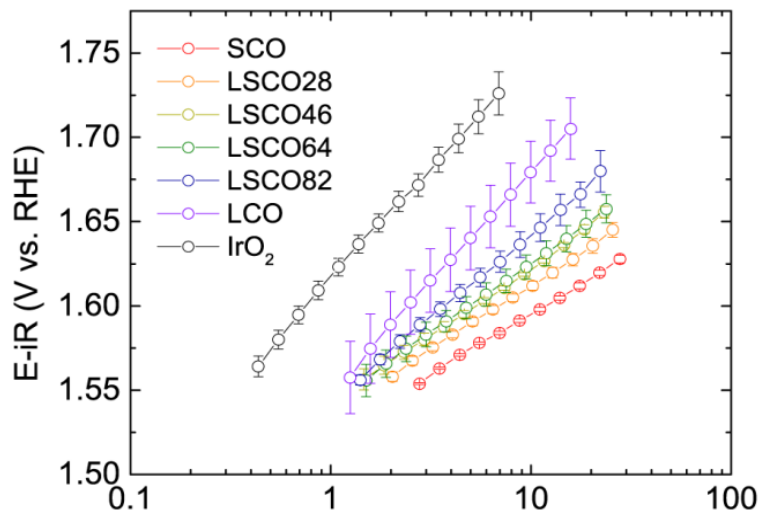
- Substituting Sr^{2+} for La^{3+} gives better control of oxygen content than thermal reduction processes
- Oxygen content is a function of both Sr^{2+} doping concentrations and charge compensation through an increase of Co oxidation state:



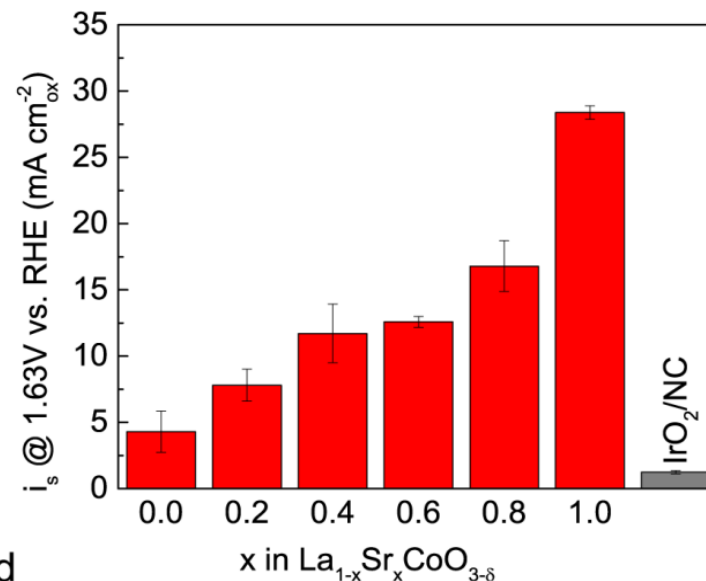
Yan, J.-Q., Zhou, J.-S. & Goodenough, J. B. Bond-length fluctuations and the spin-state transition in LCoO_3 (L=La, Pr, and Nd). *Phys. Rev. B* **69**, 134409 (2004).

OER of LSCO Samples

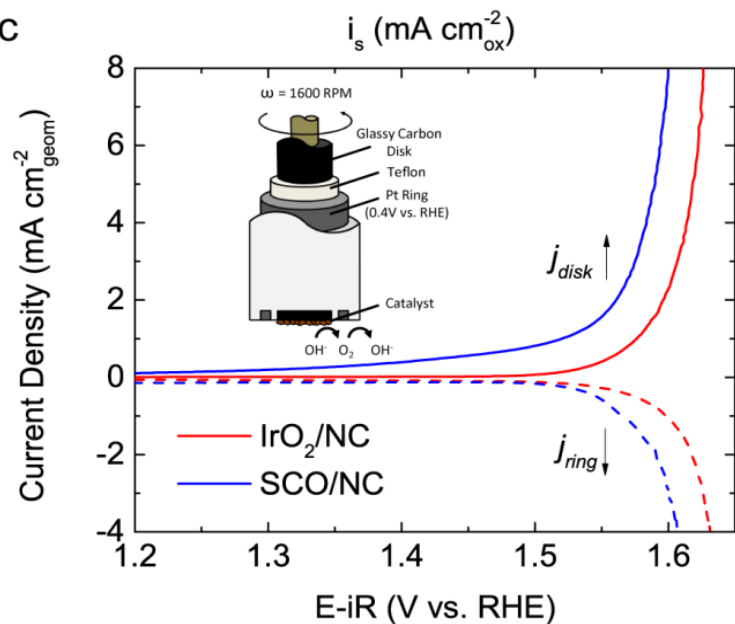
a



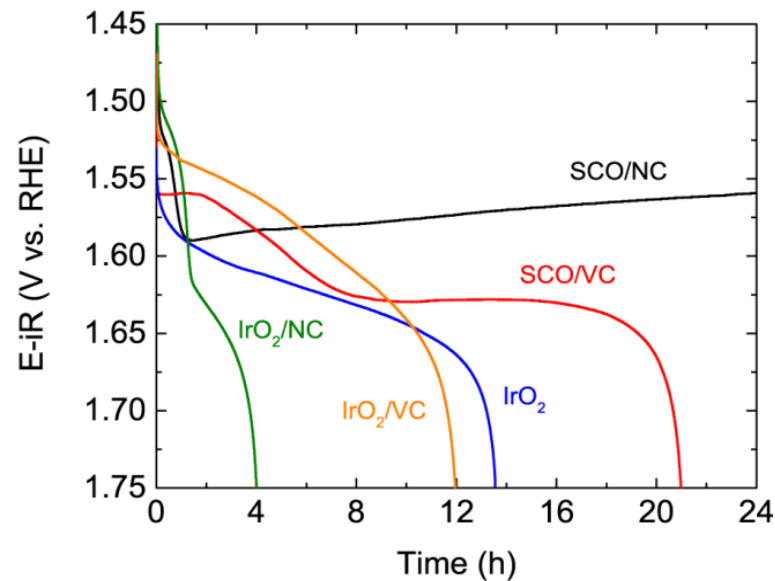
b



c

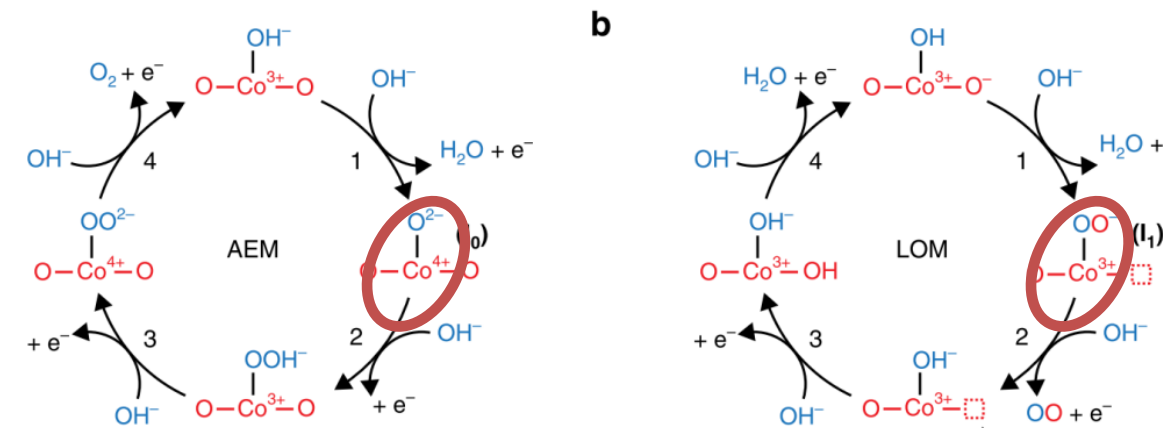


d

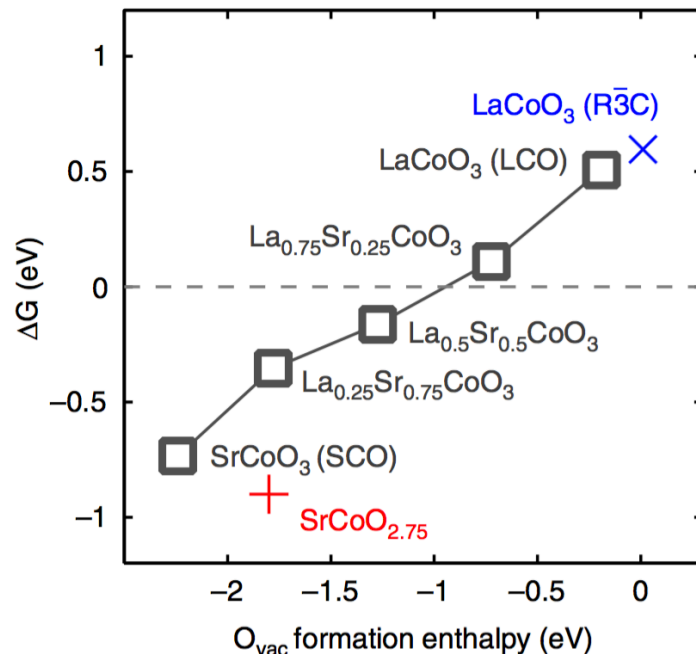
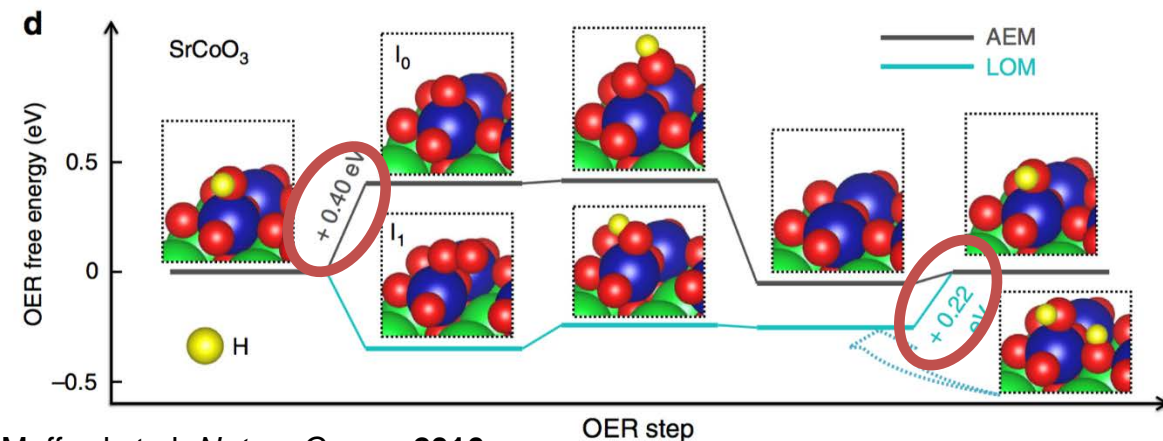
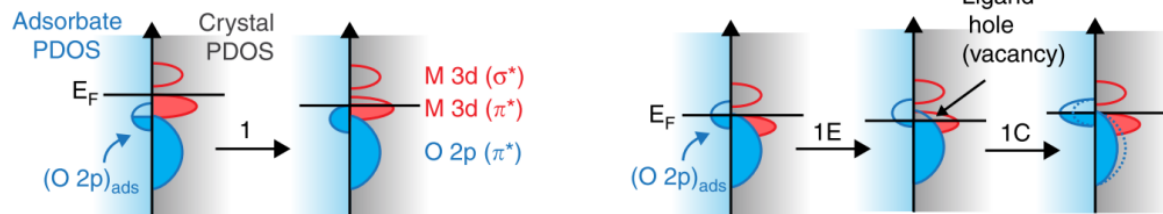


- Increase in activity with increasing Sr content

Lattice Oxygen Mediated Oxidation

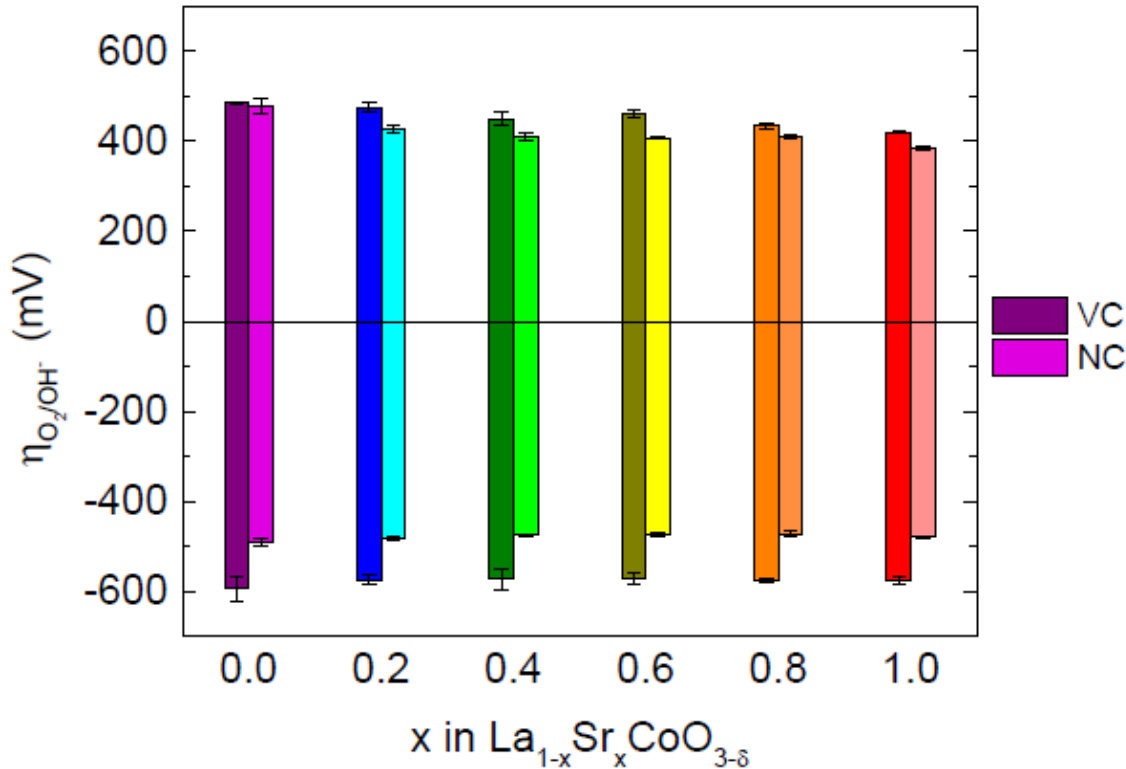


- New OER mechanism proposed, supported by DFT \rightarrow lattice oxygen mediated (LOM)
 - Lower ΔG for RDS
 - Requires M-O bond covalency
- Labile lattice oxygen experimentally shown as indicator of M-O covalency



Bifunctional OER and ORR

$\text{La}_{1-x}\text{Sr}_x\text{CoO}_{3-\delta}$ Catalysts

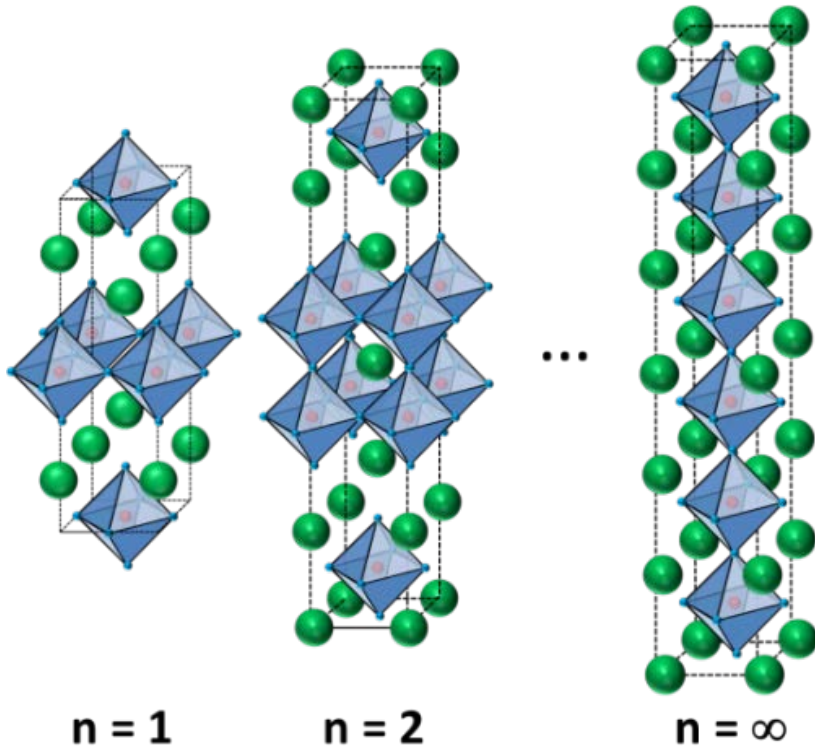


x	VC	NC
0	1.080	0.970
0.2	1.050	0.909
0.4	1.023	0.886
0.6	1.031	0.881
0.8	1.010	0.885
1	0.998	0.864

ORR @ $i_k = -3 \text{ mA/cm}^2_{\text{geom}}$
OER @ $i_k = 10 \text{ mA/cm}^2_{\text{geom}}$

Carbon is crucial in influencing oxygen electrocatalysis in bifunctional air electrodes, especially for the ORR!

What is a Ruddlesden-Popper?



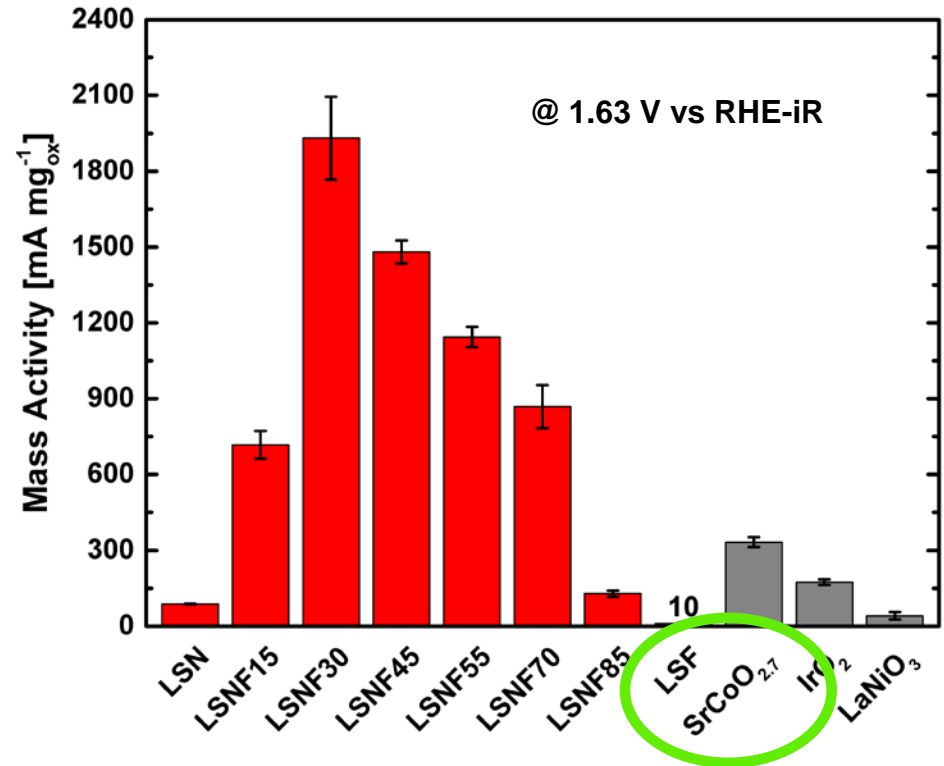
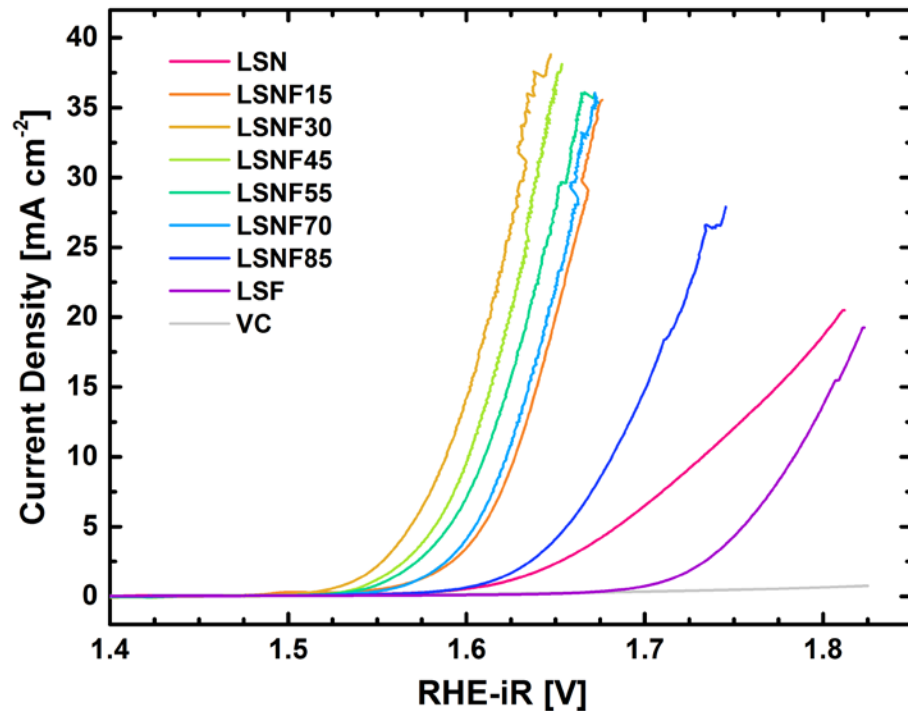
- Formula $(AO)(ABO_3)_n$
- n = perovskite layers (ABO_3) separated by a rock-salt (AO) interface
- As $n \rightarrow \infty$, RP becomes pure ABO_3 perovskite
- Location of strained AO interfaces that support Sr^{2+} substitution of La^{3+} which is unstable in a pure perovskite phase

n	Formula	A = Ln^{3+} , B $^{x+}$	A = Sr^{2+} , B $^{x+}$
1	$A_2BO_{4\pm\delta}$	2	4
n	$(AO)(ABO_3)_n$	> 2.66	4
∞	ABO_3	3	4

Ruddlesden-Popper:
 $(AO)(ABO_{3\pm\delta})_n$

RP supports structural and electronic configurations not realizable in perovskites

OER Activity of Perovskites and RP

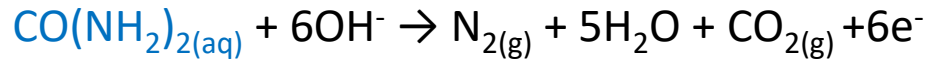


- All amounts of Fe substitution increase catalytic activity, except 100% (LSF)
- Most active composition being LSNF30 (32.7 mA cm⁻²_{ox})
- Polarization curves are averaged between anodic and cathodic scans to eliminate capacitive effects → **little to no hysteresis indicates catalyst stability**

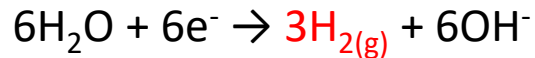
OER conditions: O₂ saturated 0.1 M KOH at 10 mV/s and 1600 rpm; 51 μg_{tot}/cm², 30 wt. % oxide on VC

Urea Oxidation Reaction

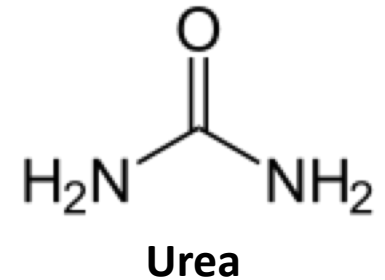
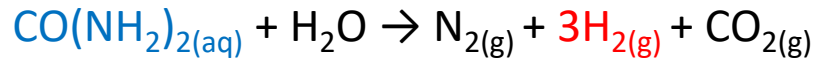
At the Anode:



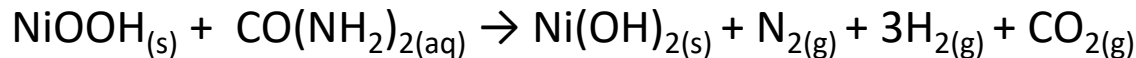
At the Cathode:



Overall:

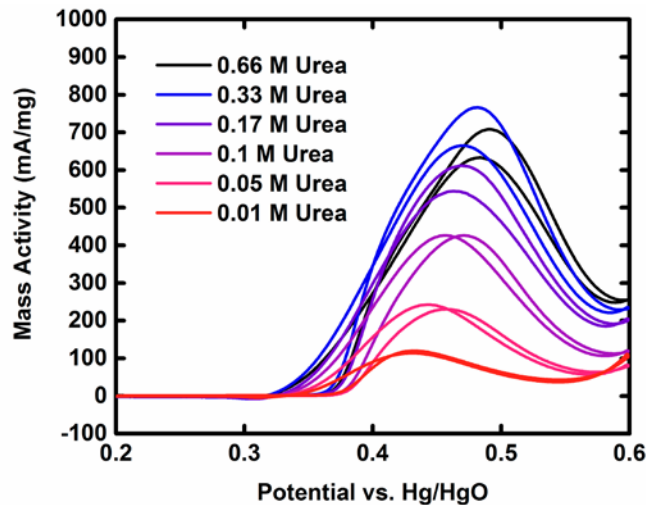
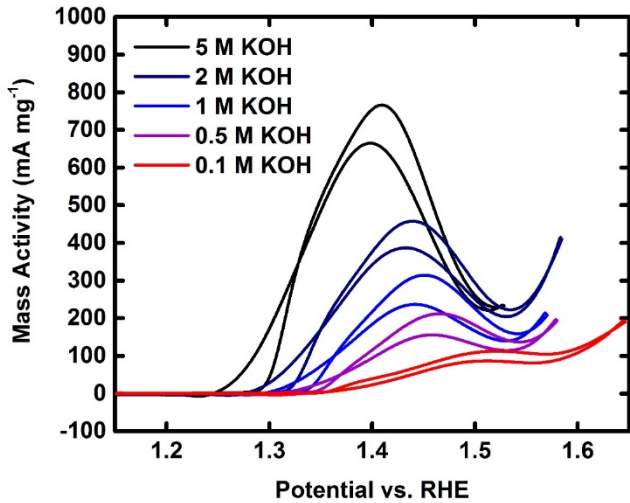


Ni metal in various morphologies used by many, EC' mechanism proposed

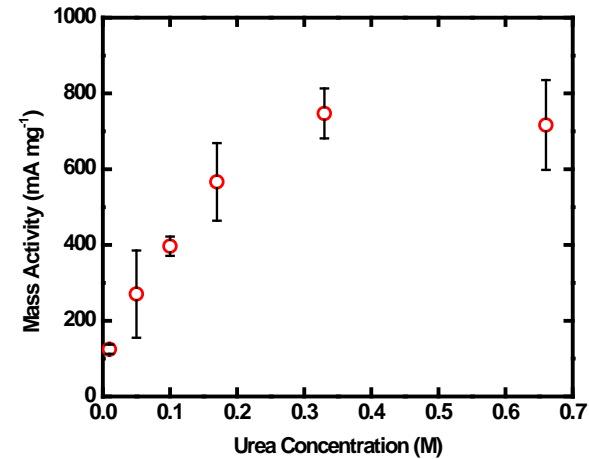
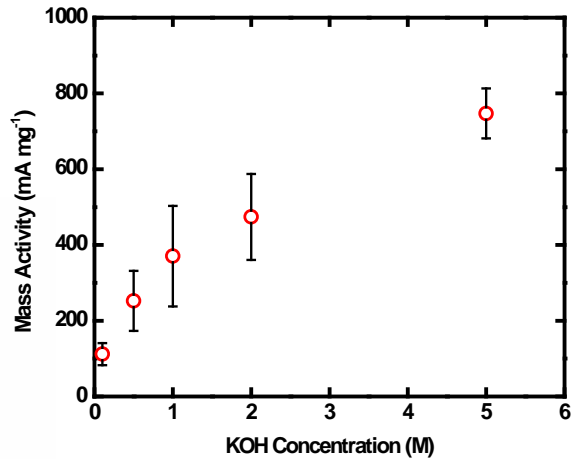


Use a material where nickel is Ni³⁺ already

LaNiO₃ Catalytic Activity



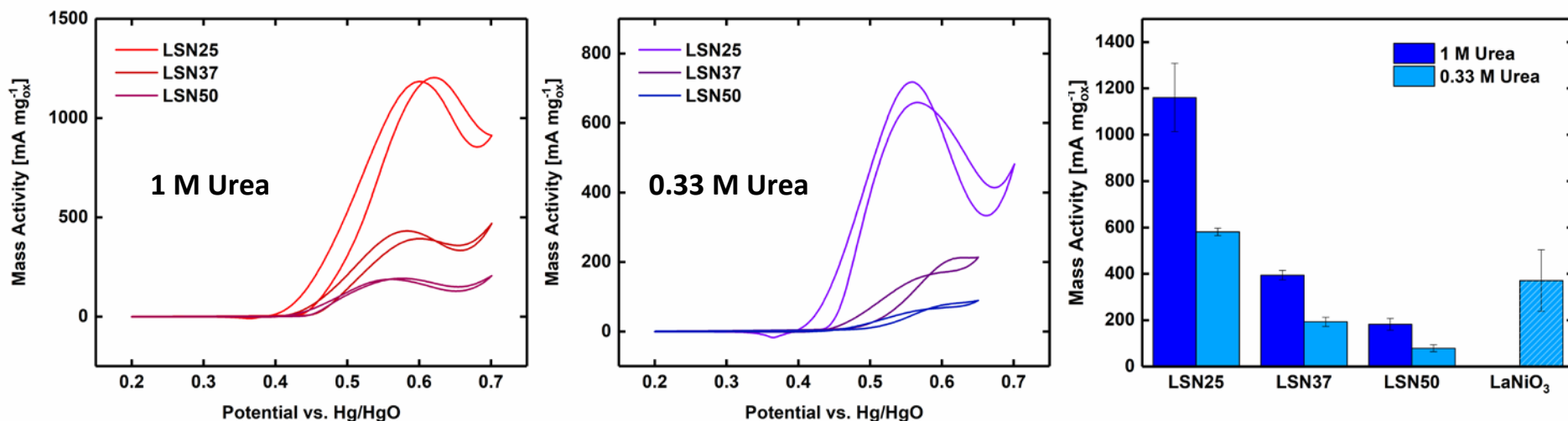
- Supported LaNiO₃ on Vulcan carbon (30 wt%) by ball-milling
- Suspended catalyst in EtOH with Na-substituted Nafion binder and drop cast onto 5 mm GCE
- Test at various concentrations of Ar-saturated KOH and urea at a scan rate of 10 mV s⁻¹



- Mass activity of 371 mA mg⁻¹ 2.25 A mg⁻¹cm⁻² in 1M KOH compared to 830 mA mg⁻¹cm⁻² in 1M KOH for NiMoO₄
- Potential shifts cathodic with increasing KOH concentration but not with increasing urea concentration
 - Supports the EC' mechanism

Urea Oxidation On LSN RP

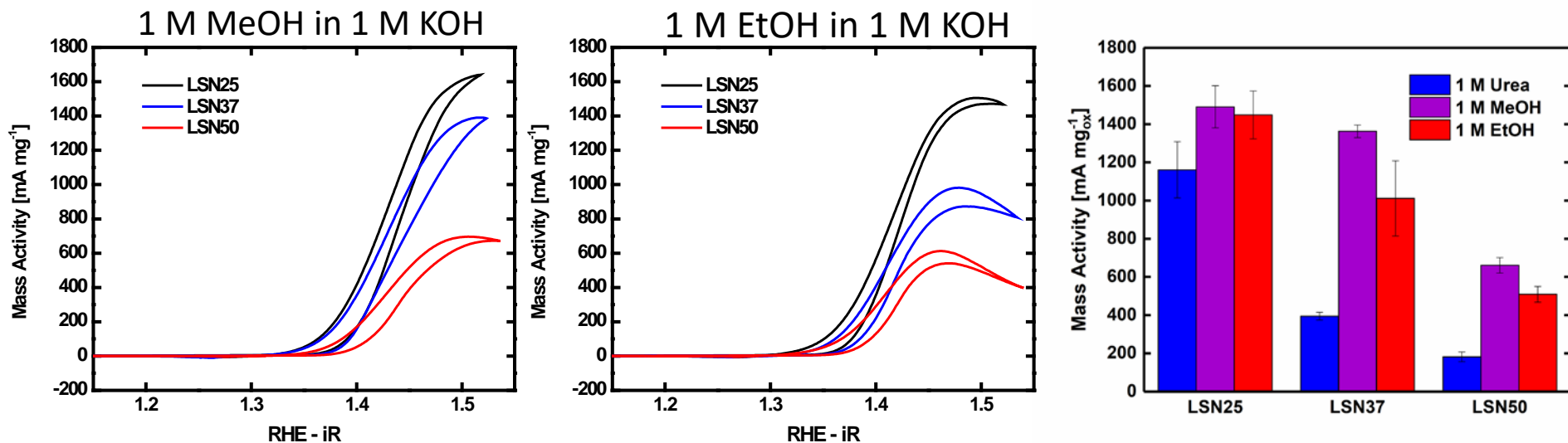
Tested in 0.33 M and 1 M urea, 1 M KOH at 10 mV s⁻¹ on stationary glassy carbon



Increasing Ni oxidation state above Ni³⁺ leads to higher activities

Material	Ni Oxidation State
LSN50	3
LSN37	3.25
LSN25	3.5

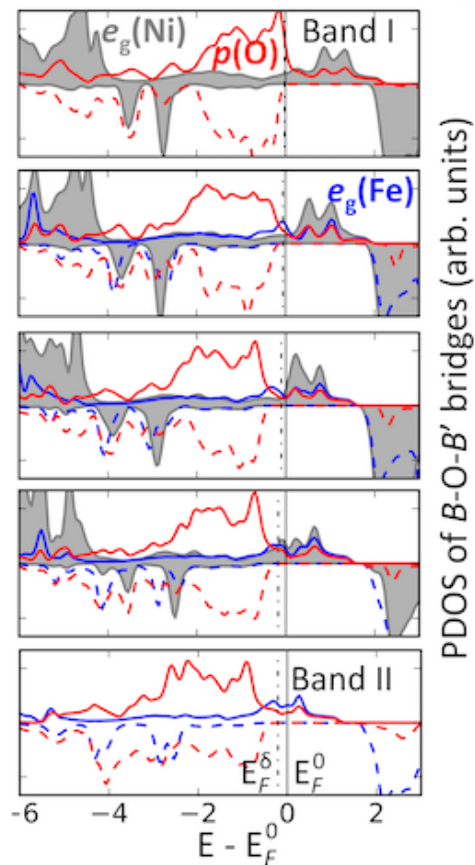
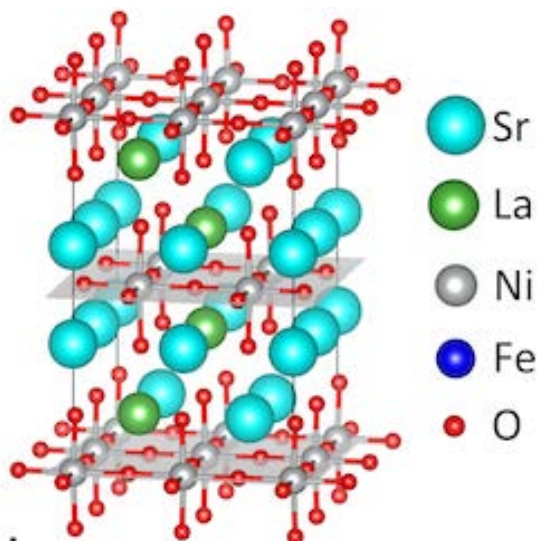
MeOH and EtOH Oxidation



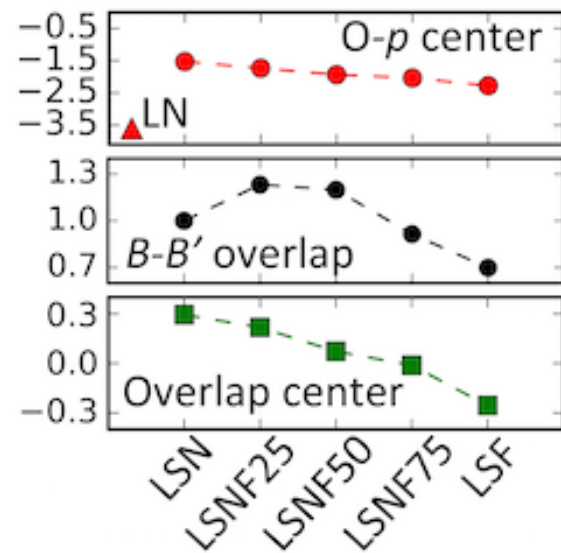
- Activities for both ethanol and methanol oxidation are extremely high
- All three reactions have similar onset potentials
 - Corresponds with Ni^{2+/3+} redox couple
 - Indicates that all three reactions (MeOH, EtOH, Urea) may follow the EC' mechanism

DFT+U Modeling On LSN RP

DFT+U to model PDOS of Ni-O-Fe bridges



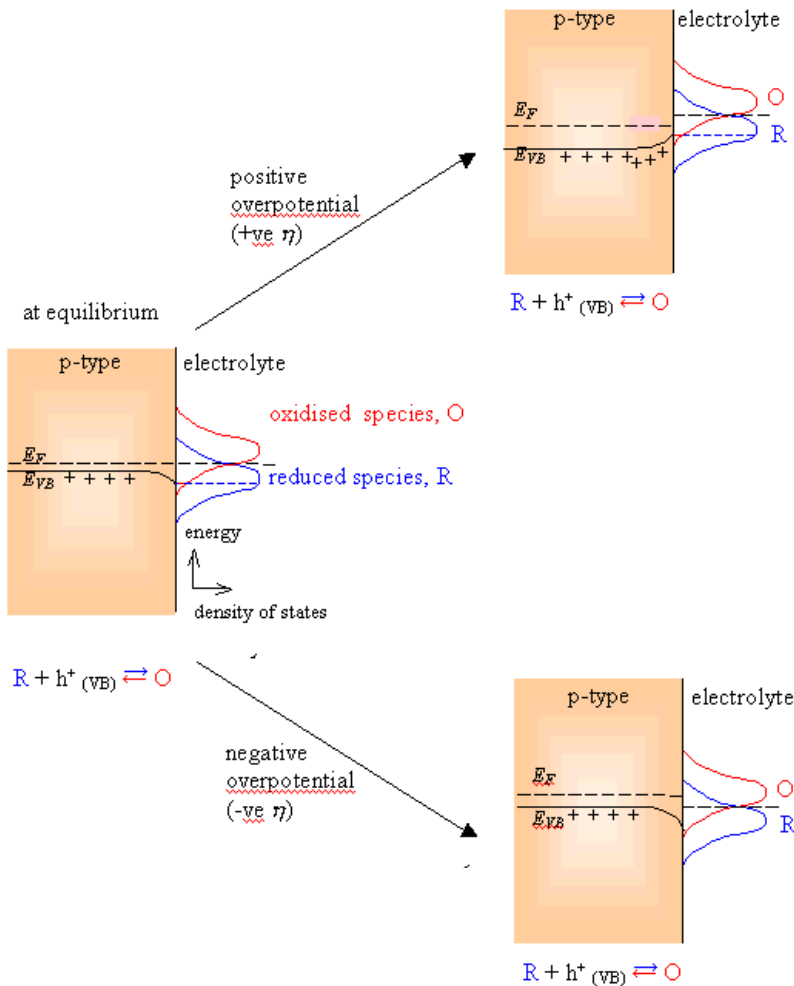
Significant overlap of the Ni e_g^* , Fe e_g^* , and O 2p bands at E_F for all compositions



Larger bandwidth \rightarrow higher density of occupied/unoccupied states around E_F \rightarrow more surface redox reactions via only slight Fermi level shift \rightarrow less energetic cost

$e_g(\text{Ni})$ and $e_g(\text{Fe})$ overlap with $p(\text{O})$ across the Fermi level: cross-gap hybridization

Marcus-Gerischer Model of ET



*Electron transfer is fastest when the electron has the same energy in the electrode as it does in **Ox** at the point of transfer. So the rate will be proportional to the DOS.*

- Probe the relationship between electronic properties and reactivity
 - Semi-conductor properties of Perovskites
 - Density of States (DOS)
 - Effects of substitution and defects
- Correlation between electronic properties and electrochemical activity
 - Structural composition
 - Electron Transfer
 - Catalytic behavior towards OER and ORR and H₂O₂ decomposition, SM oxidations

$$i_{redn} \propto k^- W_{ox}(E) C_{ox}^0 N_s(E)$$

Summary

New synthesis routes offer exquisite control of properties

Facile tuning of size, crystallinity, composition and morphology

More precise and efficient synthesis of catalysts

Reduces processing induced changes in material properties

New materials require development of advanced tools for study and elucidation of structure-property-performance

Benchmarking of Homogeneous & Heterogeneous Catalysts

Nano-sized, alloy and core@shell architectures show promise as advanced energy conversion catalysts

Need for predictive guidelines and theory

Need for activity benchmarks and standards

Explore creation of new compositions/architectures for catalysis, biosensing and environmental remediation

Promotion of catalyst synergism/bifunctionality